

## ***Drosophila* Evolution over Space and Time (DEST) - A New Population Genomics Resource**

Martin Kapun<sup>1,2,\*</sup>, Joaquin C. B. Nunez<sup>3,\*</sup>, María Bogaerts-Márquez<sup>4,\*</sup>, Jesús Murga-Moreno<sup>5,6,\*</sup>, Margot Paris<sup>7,\*</sup>, Joseph Outten<sup>3</sup>, Marta Coronado-Zamora<sup>4</sup>, Courtney Tern<sup>3</sup>, Omar Rota-Stabelli<sup>8</sup>, Maria P. García Guerreiro<sup>5</sup>, Sònia Casillas<sup>5,6</sup>, Dorcas J. Orengo<sup>9,10</sup>, Eva Puerma<sup>9,10</sup>, Maaria Kankare<sup>11</sup>, Lino Ometto<sup>12</sup>, Volker Loeschcke<sup>13</sup>, Banu S. Onder<sup>14</sup>, Jessica K. Abbott<sup>15</sup>, Stephen W. Schaeffer<sup>16</sup>, Subhash Rajpurohit<sup>17,18</sup>, Emily L. Behrman<sup>17,19</sup>, Mads F. Schou<sup>13,15</sup>, Thomas J.S. Merritt<sup>20</sup>, Brian P Lazzaro<sup>21</sup>, Amanda Glaser-Schmitt<sup>22</sup>, Eliza Argyridou<sup>22</sup>, Fabian Staubach<sup>23</sup>, Yun Wang<sup>23</sup>, Eran Tauber<sup>24</sup>, Svitlana V. Serga<sup>25,26</sup>, Daniel K. Fabian<sup>27</sup>, Kelly A. Dyer<sup>28</sup>, Christopher W. Wheat<sup>29</sup>, John Parsch<sup>22</sup>, Sonja Grath<sup>22</sup>, Marija Savic Veselinovic<sup>30</sup>, Marina Stamenkovic-Radak<sup>30</sup>, Mihailo Jelic<sup>30</sup>, Antonio J. Buendía-Ruiz<sup>31</sup>, M. Josefa Gómez-Julián<sup>31</sup>, M. Luisa Espinosa-Jimenez<sup>31</sup>, Francisco D. Gallardo-Jiménez<sup>32</sup>, Aleksandra Patenkovic<sup>33</sup>, Katarina Eric<sup>33</sup>, Marija Tanaskovic<sup>33</sup>, Anna Ullastres<sup>4</sup>, Lain Guio<sup>4</sup>, Miriam Merenciano<sup>4</sup>, Sara Guirao-Rico<sup>4</sup>, Vivien Horváth<sup>4</sup>, Darren J. Obbard<sup>34</sup>, Elena Pasyukova<sup>35</sup>, Vladimir E. Alatortsev<sup>35</sup>, Cristina P. Vieira<sup>36,37</sup>, Jorge Vieira<sup>36,37</sup>, J. Roberto Torres<sup>38</sup>, Iryna Kozeretska<sup>25,26</sup>, Oleksandr M. Maistrenko<sup>26,39</sup>, Catherine Montchamp-Moreau<sup>40</sup>, Dmitry V. Mukha<sup>41</sup>, Heather E. Machado<sup>42,43</sup>, Antonio Barbadilla<sup>5,6</sup>, Dmitri Petrov<sup>42</sup>, Paul Schmidt<sup>16</sup>, Josefa Gonzalez<sup>4</sup>, Thomas Flatt<sup>7</sup>, Alan O. Bergland<sup>3</sup>

\* equal contribution

✉ To whom correspondence should be addressed

§ The European *Drosophila* Population Genomics Consortium (DrosEU)

# The *Drosophila* Real-Time Evolution Consortium (DrosRTEC)

- 1 Department of Evolutionary Biology and Environmental Studies, University of Zürich, Switzerland
- 2 Department of Cell & Developmental Biology, Center of Anatomy and Cell Biology, Medical University of Vienna, Vienna, Austria
- 3 Department of Biology, University of Virginia, Charlottesville, USA
- 4 Institute of Evolutionary Biology, CSIC-Universitat Pompeu Fabra, Barcelona,

- Spain
- 5 Department of Genetics and Microbiology, Universitat Autònoma de Barcelona, Barcelona, Spain
  - 6 Institute of Biotechnology and Biomedicine, Universitat Autònoma de Barcelona, Barcelona, Spain
  - 7 Department of Biology, University of Fribourg, Fribourg, Switzerland
  - 8 Center Agriculture Food Environment, University of Trento, San Michele all' Adige, Italy
  - 9 Departament de Genètica, Microbiologia i Estadística, Facultat de Biologia, Universitat de Barcelona, Barcelona, Spain
  - 10 Institut de Recerca de la Biodiversitat (IRBio), Universitat de Barcelona, Barcelona, Spain
  - 11 Department of Biological and Environmental Science, University of Jyväskylä, Jyväskylä, Finland
  - 12 Department of Biology and Biotechnology, University of Pavia, Pavia, Italy
  - 13 Department of Biology, Aarhus University, Aarhus, Denmark
  - 14 Department of Biology, Hacettepe University, Ankara, Turkey
  - 15 Department of Biology, Lund University, Lund, Sweden
  - 16 Department of Biology, The Pennsylvania State University, University Park, USA
  - 17 Department of Biology, University of Pennsylvania, Philadelphia, USA
  - 18 Division of Biological and Life Sciences, School of Arts and Sciences, Ahmedabad University, Ahmedabad, India
  - 19 Janelia Research Campus, Ashburn, USA
  - 20 Department of Chemistry & Biochemistry, Laurentian University, Sudbury, Canada
  - 21 Department of Entomology, Cornell University, Ithaca, USA
  - 22 Division of Evolutionary Biology, Faculty of Biology, Ludwig-Maximilians-Universität, Munich, Germany
  - 23 Department of Evolution and Ecology, University of Freiburg, Freiburg, Germany
  - 24 Department of Evolutionary and Environmental Biology, Institute of Evolution, University of Haifa, Haifa, Israel
  - 25 Department of General and Medical Genetics, Taras Shevchenko National University of Kyiv, Kyiv, Ukraine
  - 26 State Institution National Antarctic Scientific Center, Ministry of Education and Science of Ukraine, Kyiv, Ukraine
  - 27 Department of Genetics, University of Cambridge, Cambridge, UK
  - 28 Department of Genetics, University of Georgia, Athens GA, USA
  - 29 Department of Zoology, Stockholm University, Stockholm, Sweden

- 30 Faculty of Biology, University of Belgrade, Belgrade, Serbia
- 31 IES Eladio Cabañero, Tomelloso, Spain
- 32 IES Jose de Mora, Baza, Spain
- 33 Institute for Biological Research "Siniša Stanković", National Institute of Republic of Serbia, University of Belgrade, Belgrade, Serbia
- 34 Institute of Evolutionary Biology, University of Edinburgh, UK
- 35 Institute of Molecular Genetics of the National Research Centre "Kurchatov Institute", Moscow, Russia
- 36 Instituto de Biologia Molecular e Celular (IBMC), Porto, Portugal
- 37 Instituto de Investigação e Inovação em Saúde, Universidade do Porto, Porto, Portugal
- 38 La ciència al teu món, Barcelona, Spain
- 39 Structural and Computational Biology Unit, European Molecular Biology Laboratory, Heidelberg, Germany
- 40 UMR Évolution, Génomes, Comportement et Écologie, Université Paris-Saclay, CNRS, Gif-sur-Yvette, France
- 41 Vavilov Institute of General Genetics, Russian Academy of Sciences, Moscow, Russia
- 42 Department of Biology, Stanford University, Stanford, USA
- 43 Wellcome Trust Sanger Institute, Hinxton CB10 1SA, UK

## ABSTRACT

2 *Drosophila melanogaster* is a premier model in population genetics and genomics, and a  
growing number of whole-genome datasets from natural populations of this species have  
4 been published over the last 20 years. A major challenge is the integration of these  
disparate datasets, often generated using different sequencing technologies and  
6 bioinformatic pipelines, which hampers our ability to address questions about the evolution  
and population structure of this species. Here we address these issues by developing a  
8 bioinformatics pipeline that maps pooled sequencing (Pool-Seq) reads from *D. melanogaster*  
to a hologenome consisting of fly and symbiont genomes and estimates allele frequencies  
10 using either a heuristic (PoolSNP) or a probabilistic variant caller (SNAPE-pooled). We use  
this pipeline to generate the largest data repository of genomic data available for *D.*  
12 *melanogaster* to date, encompassing 271 population samples from over 100 locations in >20  
countries on four continents. Several of these locations are sampled at different seasons  
14 across multiple years. This dataset, which we call *Drosophila Evolution over Space and*  
*Time* (DEST), is coupled with sampling and environmental meta-data. A web-based genome  
16 browser and web portal provide easy access to the SNP dataset. Our aim is to provide this  
scalable platform as a community resource which can be easily extended via future efforts  
18 for an even more extensive cosmopolitan dataset. Our resource will enable population  
geneticists to analyze spatio-temporal genetic patterns and evolutionary dynamics of *D.*  
20 *melanogaster* populations in unprecedented detail.

22 Keywords: *Drosophila melanogaster*, population genomics, SNPs, evolution, adaptation,  
demography

24

26

## Introduction

28 The vinegar fly *Drosophila melanogaster* is one of the oldest and most important genetic  
model systems and has played a key role in the development of theoretical and empirical  
30 population genetics (Schneider 2000; Hales *et al.* 2015; Haudry *et al.* 2020). Through  
decades of work, we now have a basic picture of the evolutionary origin (David and Capy  
32 1988; Lachaise *et al.* 1988; Keller 2007; Sprengelmeyer *et al.* 2020), colonization history and  
demography (Caracristi and Schlötterer 2003; Li and Stephan 2006; Duchon *et al.* 2013;  
34 Grenier *et al.* 2015; Arguello *et al.* 2019; Kapopoulou *et al.* 2020), and spatio-temporal  
diversification patterns of this species and its close relatives (Kolaczkowski *et al.* 2011;  
36 Fabian *et al.* 2012; Bergland *et al.* 2014; Lack *et al.* 2016; Machado *et al.* 2016; Kapun *et al.*  
2016, 2020). The availability of high-quality reference genomes (Adams 2000; Celniker and  
38 Rubin 2003; dos Santos *et al.* 2015) and genetic tools (Schneider 2000; Duffy 2002;  
Jennings 2011; Hales *et al.* 2015; Haudry *et al.* 2020) efficiently facilitates placing  
40 evolutionary studies of flies in a mechanistic context, allowing for the functional  
characterization of ecologically relevant polymorphism (e.g., de Jong and Bochdanovits  
42 2003; Paaby *et al.* 2010, 2014; Mateo *et al.* 2014; Kapun *et al.* 2016; Durmaz *et al.* 2018,  
2019; Ramaekers *et al.* 2019).

44 Recently, work on the evolutionary biology of *Drosophila* has been fueled by the  
growing number of population genomic datasets from field collections across a large portion  
46 of *D. melanogaster's* range (Grenier *et al.* 2015; Machado *et al.* 2019; Guirao-Rico and  
González 2019; Arguello *et al.* 2019). These genomic data consist either of re-sequenced  
48 inbred (or haploid) individuals (e.g., Mackay *et al.* 2012; Langley *et al.* 2012; Grenier *et al.*  
2015; Lack *et al.* 2015, 2016; Mateo *et al.* 2018; Kapopoulou *et al.* 2020) or pooled  
50 sequencing (Pool-Seq; e.g., Kolaczkowski *et al.* 2011; Fabian *et al.* 2012; Bastide *et al.*  
2013; Campo *et al.* 2013; Bergland *et al.* 2014; Machado *et al.* 2016, 2019; Kapun *et al.*  
52 2016, 2020) of outbred population samples. Pooled re-sequencing provides accurate and  
precise estimates of allele frequencies across most of the allele frequency spectrum (Zhu *et al.*  
54 *et al.* 2012; Lynch *et al.* 2014; Schlötterer *et al.* 2014) at a fraction of the cost of individual-  
based sequencing. Although Pool-Seq retains limited information about linkage  
56 disequilibrium (LD) relative to individual sequencing (Feder *et al.* 2012), Pool-Seq data can  
be used to infer complex demographic histories (e.g., Cheng *et al.* 2012; Bergland *et al.*  
58 2016; Deitz *et al.* 2016; Gould *et al.* 2017; Corbett-Detig and Nielsen 2017; Giesen *et al.*  
2020), characterize levels of diversity (Kofler *et al.* 2011a, 2011b; Ferretti *et al.* 2013; Kapun  
60 *et al.* 2020), and infer genomic loci involved in recent adaptation in nature (Flatt 2016; Kapun  
*et al.* 2016, 2020; Gould *et al.* 2017; Machado *et al.* 2019; Bogaerts-Márquez *et al.* 2020)  
62 and during experimental evolution (e.g. Turner *et al.* 2011; Orozco-terWengel *et al.* 2012;

Burke 2012; Kofler and Schlötterer 2014). However, the rapidly increasing number of  
64 genomic datasets processed with different bioinformatic pipelines makes it difficult to  
compare results across studies and to jointly analyze multiple datasets. Differences among  
66 bioinformatic pipelines include filtering methods for the raw reads, mapping algorithms, the  
choice of the reference genome or SNP calling approaches, potentially generating biases  
68 when combining processed datasets from different sources for joint analyses (e.g., Gautier  
*et al.* 2013; Hoban *et al.* 2016).

70 To address these issues, we have developed a modular bioinformatics pipeline to map  
Pool-Seq reads to a hologenome consisting of fly and microbial genomes, to remove reads  
72 from potential *D. simulans* contaminants, and to estimate allele frequencies using two  
complementary SNP callers. Our pipeline is available as a Docker image (available from  
74 <https://dest.bio>) to standardize versions of software used for filtering and mapping, to make  
the pipeline available independently of the operating system used and to facilitate future  
76 updates and modification of the pipeline. In addition, our pipeline allows using either  
heuristic or probabilistic methods for SNP calling, based on PoolSNP (Kapun *et al.* 2020)  
78 and SNAPE-pooled (Raineri *et al.* 2012). We also provide tools for performing *in-silico*  
pooling of existing inbred (haploid) lines that exist as part of other *Drosophila* population  
80 genomic resources (Pool *et al.* 2012; Langley *et al.* 2012; Grenier *et al.* 2015; Kao *et al.*  
2015; Lack *et al.* 2015, 2016). This pipeline is also designed to be flexible, facilitating the  
82 streamlined addition of new population samples as they arise.

Using this pipeline, we generated a unified dataset of pooled allele frequency estimates  
84 of *D. melanogaster* sampled across large portions of Europe and North America. This  
dataset is the result of the collaborative efforts of the European DrosEU (Kapun *et al.* 2020)  
86 and DrosRTEC (Machado *et al.* 2019) consortia and combines both novel and previously  
published population genomic data. Our dataset combines samples from 100 localities, 55 of  
88 which were sampled at two or more time points across the reproductive season (~10-15  
generations/year) for one or more years. Collectively, these samples represent >13,000  
90 individuals, cumulatively sequenced to >16,000x coverage. The cost-effectiveness of Pool-  
Seq has enabled us to estimate genome-wide allele frequencies over geographic space  
92 (continental and sub-continental) and time (seasonal, annual and decadal) scales, thus  
making our data a unique resource for advancing our understanding of fundamental  
94 adaptive and neutral evolutionary processes. We provide data in two file formats (VCF and  
GDS: (Danecek *et al.* 2011; Zheng *et al.* 2017), thus allowing researchers to utilize a variety  
96 of tools for computational analyses. Our dataset also contains sampling and environmental  
meta-data to enable various downstream analyses of biological interest.

98

100

102

## Materials and Methods

**Data sources.** The genomic dataset presented here has been assembled from a combination of Pool-Seq libraries and *in-silico* pooled haplotypes. We combined 246 Pool-Seq libraries of population samples from Europe, North America and the Caribbean that were sampled through space and time by two collaborating consortia in North America (DrosRTEC: <https://web.sas.upenn.edu/paul-schmidt-lab/dros-rtec/>) and Europe (DrosEU: <http://droseu.net>) between 2003 and 2016. In addition, we integrated genomic data from >900 inbred or haploid genomes from 25 populations in Africa, Europe, Australia, and North America available from the *Drosophila* Genome Nexus dataset (DGN; Lack *et al.* 2015, 2016). We further included the *D. simulans* haplotype, built as part of the DGN dataset, as an outgroup, making this repository of 272 (246 pool-seq + 25 DGN + 1 *D. simulans*) whole-genome sequenced samples the largest dataset of genome-wide SNPs available for *D. melanogaster* to date.

**Metadata.** We assembled uniform meta-data for all samples (Supplemental Material, Table S1). This information includes collection coordinates, collection date, and the number of flies per sample. Samples are also linked to bioclimatic variables from the nearest WorldClim (Hijmans *et al.* 2005) raster cell at a resolution of 2.5° and to weather stations from the Global Historical Climatology Network (GHCND; <ftp://ftp.ncdc.noaa.gov/pub/data/ghcn/daily/>) for future analysis of the environmental drivers that might underlie genetic change. We also provide summaries of basic attributes of each sample derived from the sequencing data including average read depth, PCR-duplicate rate, *D. simulans* contamination rate, relative abundances of non-synonymous versus synonymous polymorphisms ( $p_N/p_S$ ), the number of private polymorphisms, and diversity statistics (Watterson's  $\theta$ ,  $\pi$  and Tajima's  $D$ ).

126

**Sample collection.** The majority of population samples contributed by the DrosEU and the DrosRTEC consortia was collected in a coordinated fashion to generate a consistent dataset with minimized sampling bias. In brief, fly collections were performed exclusively in natural or semi-natural habitats, such as orchards, vineyards and compost piles. For most European collections, flies were collected using mashed banana, or apples with live yeast as bait in traps placed at sampling sites for multiple days to attract flies or by sweep netting (see Kapun *et al.* 2020 for more details). For North American collections, flies were collected by sweep-net, aspiration, or baiting over natural substrate or using baited traps (see Behrman *et al.* 2018; Machado *et al.* 2019 for details). Samples were either field caught flies (n=227),



136 from F1 offspring of wild caught females (n=7), from a mixture of F1 and wild caught flies  
137 (n=7), or from flies kept as isofemale lines in the lab for 5 generations or less (n=4); see  
138 Supplemental Table 1 for more information. To minimize cross-contamination with the  
139 closely related sympatric sister species *D. simulans*, we only sequenced male *D.*  
140 *melanogaster* specimens, allowing for higher confidence discrimination between the two  
141 species based on the morphology of male genitalia (Capy and Gibert 2004; Markow and  
142 O'Grady 2005). Samples were stored in 95% ethanol at -20°C before DNA extraction.

144 **DNA extraction and sequencing.** The DrosEU and DrosRTEC consortia centralized  
145 extractions from pools of flies. DNA was extracted either using chloroform/phenol-based  
146 (DrosEU: Kapun *et al.* 2020) or lithium chloride/potassium acetate extraction protocols  
147 (DrosRTEC: Bergland *et al.* 2014; Machado *et al.* 2019) after homogenization with bead  
148 beating or a motorized pestle. DrosEU samples from the 2014 collection were sequenced on  
149 an Illumina NextSeq 500 sequencer at the Genomics Core Facility of Pompeu Fabra  
150 University in Barcelona, Spain. Libraries of the previously unpublished DrosEU samples  
151 from 2015 and 2016 were constructed using the Illumina TruSeq PCR Free library  
152 preparation kit following the manufacturer's instructions and sequenced on the Illumina  
153 HiSeq X platform as paired-end fragments with 2 x 150 bp length at NGX Bio (San  
154 Francisco, California, USA). The previously published samples of the DrosRTEC consortium  
155 were prepared and sequenced on GAIIIX, HiSeq2000 or HiSeq3000 platforms, as described  
156 in Bergland *et al.* (2014) and Machado *et al.* (2019). For information on DNA extraction and  
157 sequencing methods of the various DGN samples see Lack *et al.* (2016).

158  
159 **Mapping pipeline.** The joint analysis of genomic data from different sources requires the  
160 application of uniform quality criteria and a common bioinformatics pipeline. To accomplish  
161 this, we developed a standardized pipeline that performs filtering, quality control and  
162 mapping of any given Pool-Seq sample (see Supplemental Information Figure S1). This  
163 pipeline performs quality filtering of raw reads, maps reads to a hologenome (see below),  
164 performs realignment and filtering around indels, and filters for mapping quality. The output  
165 of this pipeline includes quality control metrics, bam files, pileup files, and allele frequency  
166 estimates for every site in the genome (gSYNC, see below). Our pipeline is provided as a  
167 Docker image, which automatically installs external software and executes the pipeline  
168 across various operating systems. Our pipeline will facilitate the integration of future samples  
169 to extend the worldwide *D. melanogaster* SNP dataset presented here.

170 The mapping pipeline includes the following major steps. Prior to mapping, we removed  
171 sequencing adapters and trimmed the 3' ends of all reads using cutadapt (Martin 2011). We  
172 enforced a minimum base quality score  $\geq 18$  (-q flag in cutadapt) and assessed the quality of



raw and trimmed reads with FASTQC (Andrews 2010). Trimmed reads with minimum length  
174 < 75 bp were discarded and only intact read pairs were considered for further analyses.  
Overlapping paired-end reads were merged using *bbmerge* (v. 35.50; (Bushnell *et al.* 2017).  
176 Trimmed reads were mapped against a compound reference genome (“hologenome”)  
consisting of the genomes of *D. melanogaster* (v.6.12) and *D. simulans* (Hu *et al.* 2013) as  
178 well as genomes of common commensals and pathogens, including *Saccharomyces*  
*cerevisiae* (GCF\_000146045.2), *Wolbachia pipientis* (NC\_002978.6), *Pseudomonas*  
180 *entomophila* (NC\_008027.1), *Commensalibacter intestine* (NZ\_AGFR00000000.1),  
*Acetobacter pomorum* (NZ\_AEUP00000000.1), *Gluconobacter morbifer*  
182 (NZ\_AGQV00000000.1), *Providencia burhodogranariea* (NZ\_AKKL00000000.1),  
*Providencia alcalifaciens* (NZ\_AKKM01000049.1), *Providencia rettgeri*  
184 (NZ\_AJSB00000000.1), *Enterococcus faecalis* (NC\_004668.1), *Lactobacillus brevis*  
(NC\_008497.1), and *Lactobacillus plantarum* (NC\_004567.2), using *bwa mem* (v. 0.7.15; Li  
186 2013) with default parameters. We retained reads with mapping quality greater than 20 and  
reads with no secondary alignment using *samtools* (Li *et al.* 2009). PCR duplicate reads  
188 were removed using *Picard MarkDuplicates* (v.1.109; <http://picard.sourceforge.net>).  
Sequences were re-aligned in the proximity of insertions-deletions (indels) with GATK (v3.4-  
190 46; McKenna *et al.* 2010). We identified and removed any reads that mapped to the *D.*  
*simulans* genome using a custom python script, following methods outlined previously  
192 (Machado *et al.* 2019; Kapun *et al.* 2020; for a more in-depth analysis of *D. simulans*  
contamination see Wallace *et al.* 2020).

194

**Incorporation of the DGN dataset.** We incorporated population allele frequency estimates  
196 derived from inbred-line and haploid embryo sequencing data from populations sampled  
throughout the world. These samples have been previously collected and sequenced by  
198 several groups (Pool *et al.* 2012; Langley *et al.* 2012; Grenier *et al.* 2015; Kao *et al.* 2015;  
Lack *et al.* 2015, 2016) and form the *Drosophila* Genome Nexus dataset (DGN; Lack *et al.*  
200 2015, 2016). We included 25 DGN populations with  $\geq 5$  individuals per population, plus the  
*D. simulans* haplotype built as part of the DGN dataset. The DGN populations that we used  
202 are primarily from Africa (n=18) but also include populations from Europe (n=2), North  
America (n=3), Australia (n=1), and Asia (n=1).

204 To incorporate the DGN populations into the DrosEU and DrosRTEC Pool-Seq  
datasets, we used the pre-computed FASTA files (“Consensus Sequence Files” from  
206 <https://www.johnpool.net/genomes.html>) and calculated allele frequencies at every site, for  
each population, using custom *bash* scripts. We calculated allele frequencies per population  
208 by summing reference and alternative allele counts across all individuals. Since estimates of  
allele frequencies and total allele counts for the DGN samples only consider unambiguous

210 IUPAC codes, heterozygous sites or sites masked as N's in the original FASTA files were  
converted to missing data. We used *liftover* (Kuhn *et al.* 2013) to translate genome  
212 coordinates to *Drosophila* reference genome release 6 (dos Santos *et al.* 2015) and  
formatted them to match the gSYNC format (described below).

214

**SNP calling strategies.** We used two complementary approaches to perform SNP calling.  
216 The first was PoolSNP (Kapun *et al.* 2020), a heuristic tool which identifies polymorphisms  
based on the combined evidence from multiple samples. This approach is similar to other  
218 common Pool-Seq variant calling tools (Koboldt *et al.* 2009, 2012; Kofler *et al.* 2011a,  
2011b). PoolSNP integrates allele counts across multiple independent samples and applies  
220 stringent minor allele count and minor allele frequency thresholds for variant detection.  
PoolSNP is expected to be good at detecting variants present in multiple populations, but is  
222 not very sensitive to rare private alleles. The second approach was SNAPE-pooled (Raineri  
*et al.* 2012), a Bayesian tool which identifies polymorphic sites for each population  
224 independently using pairwise nucleotide diversity estimates as a prior. SNAPE-pooled is  
expected to be more sensitive to rare private polymorphisms, but also might have a higher  
226 false positive rate for variant detection.

228 **gSYNC generation and filtering.** Our pipeline utilizes a common data-format (SYNC; Kofler  
*et al.* 2011b) to encode allele counts for each population sample. A "genome-wide SYNC"  
230 (gSYNC) file records the number of A,T,C, and G for every site of the reference genome.  
Because gSYNC files for all populations have the same dimension, they can be quickly  
232 combined and passed to a SNP calling tool. They can be filtered and are also relatively  
small for a given sample (~500Mb), enabling efficient data sharing and access. The gSYNC  
234 file is analogous to the gVCF file format as part of the GATK HaplotypeCaller approach  
(McKenna *et al.* 2010) but is specifically tailored to Pool-Seq samples.

236 To generate a Pool-SNP gSYNC file, we first converted BAM files to the MPILEUP  
format with *samtools mpileup* using the -B parameter to suppress recalculations of per-base  
238 alignment qualities and filtered for a minimum mapping quality with the parameter -q 25.  
Next, we converted the MPILEUP file containing mapped and filtered reads to the gSYNC  
240 format using custom python scripts, which are available at <https://dest.bio>. To generate a  
SNAPE-pooled gSYNC file, we ran the SNAPE-pooled version specific to Pool-Seq data for  
242 each sample with the following parameters:  $\theta=0.005$ ,  $D=0.01$ , prior='informative',  
fold='unfolded' and nchr=number of flies (x2 for autosomes and x1 for the X chromosome)  
244 following Guirao-Rico and Gonzalez (2021). We converted the SNAPE-pooled output file to  
a gSYNC file containing the counts of each allele per position and the posterior probability of  
246 polymorphism as defined by SNAPE-pooled using custom python scripts. We only

248 considered positions with a posterior probability  $\geq 0.9$  as being polymorphic and with a  
posterior probability  $\leq 0.1$  as being monomorphic. In all other cases, positions were marked  
as missing data.

250 We masked gSYNC files for Pool-SNP and SNAPE-pooled using a common set of  
filters. Sites were filtered from gSYNC files if they had: (1) minimum read depth  $< 10$ ; (2)  
252 maximum read depth  $>$  the 95% coverage percentile of a given chromosomal arm and  
sample; (3) located within repetitive elements as defined by RepeatMasker; (4) within 5 bp  
254 distance up- and downstream of indel polymorphisms identified by the GATK IndelRealigner.  
Filtered sites were converted to missing data in the gSYNC file. The location of masked  
256 positions for every sample was recorded as a BED file.

258 **VCF generation.** We combined the masked PoolSNP-gSYNC files into a two-dimensional  
matrix, where rows correspond to each position in the reference genome and columns  
260 describe chromosome, position and reference allele, followed by allele counts in SYNC  
format for every sample in the dataset. This combined matrix was then subjected to variant  
262 calling using PoolSNP, resulting in a VCF formatted file. We performed SNP calling only for  
the major chromosomal arms (X, 2L, 2R, 3L, 3R) and the 4th (dot) chromosome.

264 We first evaluated the choice of two heuristic parameters applied to PoolSNP: global  
minor allele count (MAC) and global minor allele frequency (MAF). Using all 272 samples,  
266 we varied MAF (0.001, 0.01, 0.05) and MAC (5-100) and called SNPs at a randomly  
selected 10% subset of the genome. We calculated  $p_N/p_S$  and used this value to tune our  
268 choice of MAF and MAC. We found that a global MAF=0.001 and a global MAC=50 provided  
reasonable estimates of  $p_N/p_S$  for all populations. We therefore used these parameters for  
270 genome-wide variant calling (see *Results*: Identification and quality control of SNPs). We  
kept a third heuristic parameter, the missing data rate, constant at a minimum of 50%.

272 We generated three versions of the variant files, which differ in their inclusion of the  
DGN samples and the SNP calling strategy. For PoolSNP variant calling, we generated two  
274 variant tables: the first version incorporates all 272 samples of the Pool-Seq (DrosRTEC,  
DrosEU) and *in-silico* Pool-Seq populations (DGN). The second version only considers the  
276 246 Pool-Seq samples. We combined masked SNAPE-pooled gSYNC files into a two-  
dimensional matrix, as described above, and generated a VCF formatted output based on  
278 allele counts for any site found to be polymorphic in one or more populations. Based on this  
dataset we then generated a SNAPE-pooled VCF file, which included the 246 Pool-Seq  
280 samples. Final VCF files were annotated with SNPeff (version 4.3; Cingolani *et al.* 2012) and  
stored in VCF and BCF (Danecek *et al.* 2011) file formats alongside an index file in TABIX  
282 format (Li 2011). Besides VCF files, we also stored SNP data in the GDS file format using  
the *R* package SeqArray (Zheng *et al.* 2017).

284

**Population genetic analyses.** We estimated allele frequencies for each site across  
286 populations as the ratio of the alternate allele count to the total site coverage. We also  
calculated per-site averages for nucleotide diversity ( $\pi$ , Nei 1987), Watterson's  $\theta$  (Watterson  
288 1975) and Tajima's  $D$  (Tajima 1989) across all sites or in non-overlapping windows of 100  
kb, 50 kb and 10 kb length. To estimate these summary statistics, we converted masked  
290 gSYNC files (with positions filtered for repetitive elements, low and high read depth, and  
proximity to indels; see *gSYNC generation and filtering*) back to the mpileup format using  
292 custom-made scripts. mpileup files were processed using npstat v.1 (Ferretti *et al.* 2013)  
with parameters -maxcov 10000 and -nolowfreq m=0 in order to include all filtered positions  
294 for analysis. We only considered sites identified as being polymorphic by PoolSNP or  
SNAPE-pooled for analysis, using the -snppile option of npstat. For the DGN populations,  
296 chromosomes-wide summary statistics were estimated only for samples with less than 50%  
missing data per chromosome. Due to small sample sizes, Tajima's  $D$  was not estimated for  
298 7 African DGN populations that consisted of only 5 haploid embryos. In addition, we  
calculated  $p_N/p_S$  ratios based on SNP annotations with SNPeff (Cingolani *et al.* 2012) using  
300 a custom-made python script. To compare population genetic estimates between the  
PoolSNP versus SNAPE-pooled datasets, we performed Pearson's correlations on the 210  
302 populations present in both datasets (see Identification and quality control of SNPs) using  
the stats package of R v. 3.6.3. The effects of pool size (number of individuals sampled per  
304 population) on genome-wide estimates of  $\pi$ , Watterson's  $\theta$ , Tajima's  $D$  and  $p_N/p_S$  estimates  
were examined for European and North American populations using the PoolSNP dataset  
306 and a generalized linear model (GLM) in R v3.6.3. Finally, for 48 European populations we  
estimated Pearson's correlations between  $\pi$ , Watterson's  $\theta$  and Tajima's  $D$  as estimated  
308 from the PoolSNP dataset versus previous estimates by Kapun *et al.* (2020) using the stats  
package of R v3.6.3.

310 Next, we examined patterns of between-population differentiation by calculating  
window-wise estimates of pairwise  $F_{ST}$ , based on the method from Hivert *et al.* (2018)  
312 implemented in the computePairwiseFSTmatrix() function of the R package poolfstat  
(v1.1.1). This analysis was performed for the dataset composed of 271 samples processed  
314 with PoolSNP, focusing on SNPs shared across the whole dataset. Finally, we averaged  
pairwise  $F_{ST}$  within and among phylogenetic clusters (Africa [17 samples], North America [76  
316 samples], Eastern Europe [83 samples] and Western Europe [93 samples]; not included:  
China and Australia). These  $F_{ST}$  tracks at windows sizes of 100kb, 50kb and 10kb are  
318 available at <https://dest.bio> (Supplemental Figures S2, S3).

To assess population structure in the worldwide dataset, we applied PCA, population  
320 clustering, and population assignment based on a discriminant analysis of principal

components (DAPC; Jombart *et al.* 2010) to all 271 PoolSNP-processed samples. For these  
322 analyses, we subsampled a set of 100,000 SNPs spaced apart from each other by at least  
500 bp. We optimized our models using cross-validation by iteratively dividing the data as  
324 90% for training and 10% for learning. We extracted the first 40 PCs from the PCA and ran  
Pearson's correlations between each PC and all loci. We subsequently extracted the top  
326 33,000 SNPs with large and significant correlations to PCs 1-40. We chose the 33,000  
number as a compromise between panel size and differentiation power. For example,  
328 depending on the number of individuals surveyed, these 33,000 DIMs can discern  
divergence ( $\tau$ ) between two populations with parametric  $F_{ST}$  of 0.001- 0.0001 for sample  
330 sizes ( $n$ ) of 10-1000. These estimates come from the phase change formula:  $\tau \approx F_{ST} =$   
 $1/(nm)^{1/2}$  (Patterson *et al.* 2006). Here, the two populations were sampled for  $n/2$  individuals  
332 and genotyped at  $m=33,000$  markers. Furthermore, we included SNPs as a function of the  
%VE of each PC. PCAs, clustering, and assignment-based DAPC analyses were carried out  
334 using the *R* packages FactoMiner (v. 2.3), factoextra (v. 1.0.7) and adegenet (v. 2.1.3),  
respectively.

336

**Web-based genome browser.** Our HTML-based DEST browser (Supplemental Information  
338 Figure S2) is built on a JBrowse Docker container (Buels *et al.* 2016), which runs under  
Apache on a CentOS 7.2 Linux x64 server with 16 Intel Xeon 2.4 GHz processors and 32  
340 GB RAM. It implements a hierarchical data selector that facilitates the visualization and  
selection of multiple population genetic metrics or statistics for the 272 samples based on  
342 the PoolSNP-processed dataset, taking into account sampling location and date.  
Importantly, our genome browser provides a portal for downloading allelic information and  
344 pre-computed population genetics statistics in multiple formats (Supplemental Information  
Figures 2A+C, S3), a usage tutorial (Supplemental Information Figure S2B) and versatile  
346 track information (Supplemental Information Figure S2D). Bulk downloads of full variation  
tracks are available in BigWig format (Kent *et al.* 2010) and Pool-Seq files (in VCF format)  
348 are downloadable by population and/or sampling date using custom options from the Tools  
menu (Supplemental Information Figure S2C). All data, tools, and supporting resources for  
350 the DEST dataset, as well as reference tracks downloaded from FlyBase (v.6.12) (dos  
Santos *et al.* 2015), are freely available at <https://dest.bio>.

352

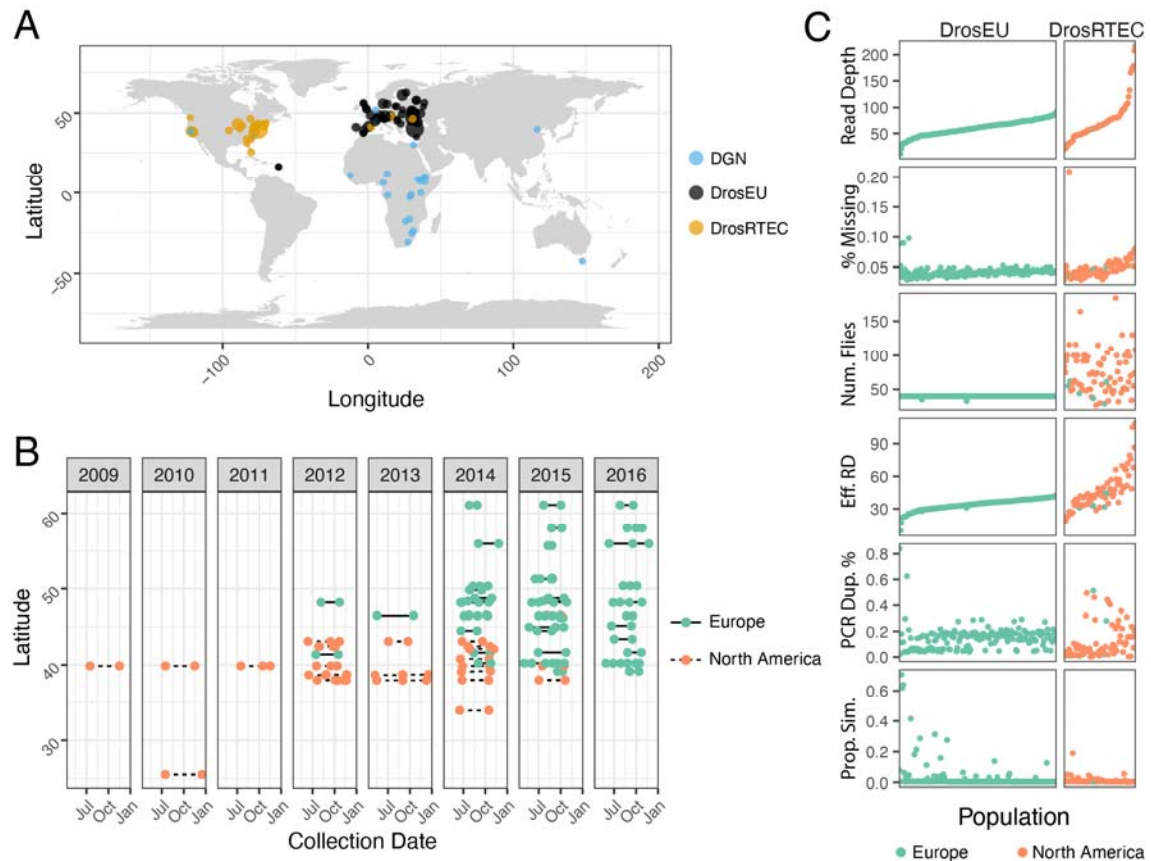
354

## Results and Discussion

**Integrating a worldwide collection of *D. melanogaster* population genomics  
356 resources.** We developed a modular and standardized pipeline for generating allele



frequency estimates from pooled resequencing of *D. melanogaster* genomes (Supplemental Figure 1). Using this pipeline, we assembled a dataset of allele frequencies from 271 *D. melanogaster* populations sampled around the world (Figure 1A, Supplemental Material, Table S1). Many of these samples were collected at the same location, at different seasons and over multiple years (Figure 1B). The nature of the genomic data for each population varies as a consequence of biological origin (e.g., inbred lines or Pool-Seq), library preparation method, and sequencing platform.



364 **Figure 1.** Sampling location, dates, and quality metrics. (A) Map showing the 271 sampling localities  
 366 forming the DEST dataset. Colors denote the datasets that were combined together. (B) Collection  
 368 dates for localities sampled more than once. (C) General sample features of the DEST dataset. The  
 x-axis represents the population sample, ordered by the average read depth.

370 To assess whether these features affect basic attributes of the dataset, we calculated six  
 372 basic quality metrics (Figure 1C, Supplemental Material, Table S2). On average, median  
 374 read depth across samples is 62X (DGN samples range: 1-190X; Pool-Seq samples range:  
 10-217X). Missing data rates were less than 7% for most (95%) of the samples. Excluding  
 populations with high missing data rate (>7%), the proportion of sites with missing data was  
 positively correlated with read depth ( $p=1.2 \times 10^{-9}$ ,  $R^2=0.4$ ). The positive correlation between

376 read depth and missing data rate is surprising and likely a consequence of masking sites  
with high coverage. The number of flies per sample varied from 40 to 205, with considerable  
378 heterogeneity among the DrosRTEC samples (standard deviation [sd] = 30), but not among  
DrosEU samples (sd = 0.04). Variation in the number of flies and in sequencing depth is  
380 reflected in the effective read depth, an estimate of the number of independent reads after  
accounting for double binomial sampling that occurs during PoolSeq (Eff. RD; Kolaczkowski  
382 *et al.* 2011; Feder *et al.* 2012; Figure 1C). There was considerable variation in PCR  
duplicate rate among samples, with notable differences between batches of DrosEU  
384 samples (~6% in 2014 vs. 18% in 2015/16; t-test  $p=1.8 \times 10^{-19}$ ) and DrosRTEC samples (~3%  
in samples collected as part of Bergland *et al.* (2014) vs. ~14% in samples collected as part  
386 of Machado *et al.* (2019;  $p=6.37 \times 10^{-3}$ ). Curiously, the 2015/2016 DrosEU samples were  
made with a PCR-free kit, suggesting that the observed PCR duplicates were optical  
388 duplicates and not amplification artifacts. Contamination of samples by *D. simulans* varied  
among populations but was generally absent (<1% *D. simulans* specific reads).

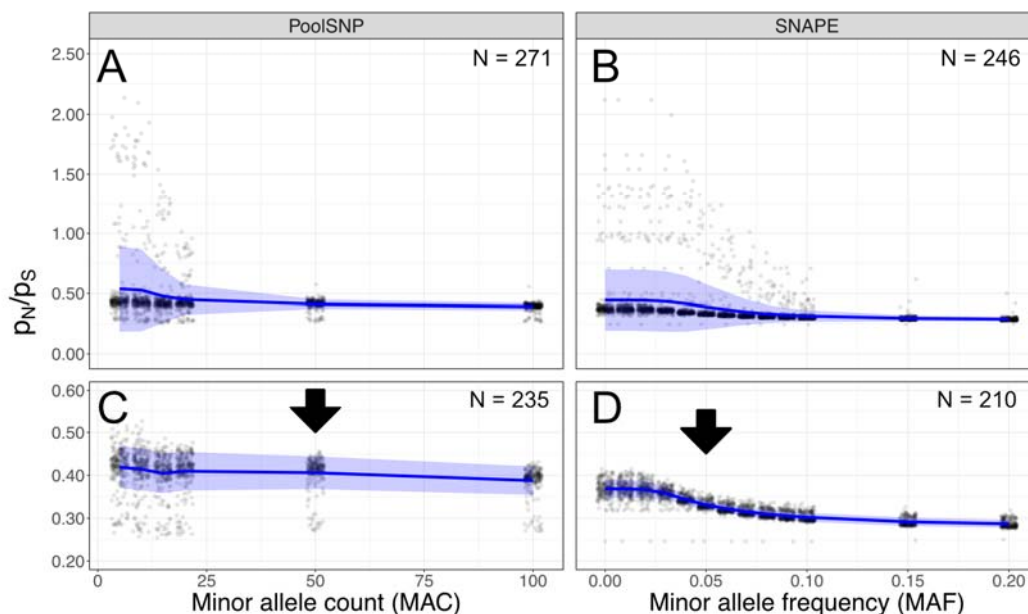
390

**Identification and quality control of SNPs.** In order to determine appropriate SNP calling  
392 and filtering parameters, and to identify potentially problematic population samples, we first  
calculated the ratio of non-synonymous to synonymous polymorphism ( $p_N/p_S$ ) for each  
394 population sample. We chose this metric because it can reflect the presence of sequencing  
errors that would disproportionately inflate  $p_N$  relative to  $p_S$ .

396 For the PoolSNP dataset, we varied the global minor allele count (MAC) and global  
minor allele frequency (MAF) and then calculated  $p_N/p_S$ . We observed that  $p_N/p_S$  was  
398 negatively correlated with MAC (linear regression;  $p < 0.001$ ; Figure 2A). MAC thresholds <50  
resulted in large variances of  $p_N/p_S$  caused by 36 populations characterized by unusually  
400 high  $p_N/p_S$  ratios (Supplemental Material, Table S3; Figures 2A and 2C). Some (n=21) of  
these samples had previously been found to show positive values of Tajima's *D* across the  
402 whole genome (Kapun *et al.* 2020) and are characterized by a large number of private  
polymorphisms (Supplemental Material, Table S3; see below), indicating that there may be  
404 elevated numbers of sequencing errors in some samples. Applying a MAC threshold of 50  
reduced the elevated  $p_N/p_S$  ratios to values similar to the rest of the dataset, and suggesting  
406 that the potential sequencing errors had been largely removed. To minimize false positive  
variant calling, we therefore conservatively chose MAC=50 and MAF=0.001 as threshold  
408 parameters for SNP calling with PoolSNP. Using these parameters, we identified 4,381,144  
polymorphisms segregating among the 271 *D. melanogaster* samples (Pool-Seq plus DGN),  
410 and 4,042,456 polymorphisms segregating among the 246 Pool-Seq samples (excluding  
DGN), using PoolSNP.



412 SNAPE calls variants in each sample separately using a probabilistic approach, in  
contrast to PoolSNP, which integrates allelic information across all populations for heuristic  
414 SNP calling. To quantify the amount of putative sequencing errors among low frequency  
variants we varied the local MAF threshold per sample and calculated  $p_N/p_S$  for each sample  
416 in the SNAPE-pooled dataset. Similar to PoolSNP, we found that elevated  $p_N/p_S$  was  
negatively correlated with a local MAF threshold (linear regression;  $p < 0.001$ ; Figure 2B) and  
418 that the 36 above-mentioned problematic samples also had a strong effect on the variance  
and mean of  $p_N/p_S$  ratios. Accordingly, we removed these 36 samples and applied a  
420 conservative MAF filter of 5% for the remainder of the SNAPE-pooled analysis. Our results  
identified 8,541,651 polymorphisms segregating among the remaining 210 samples. Below,  
422 we discuss the geographic distribution and global frequency of SNPs identified using these  
two methods in order to provide insight into the stark discrepancy in the number of SNPs  
424 that they identify.



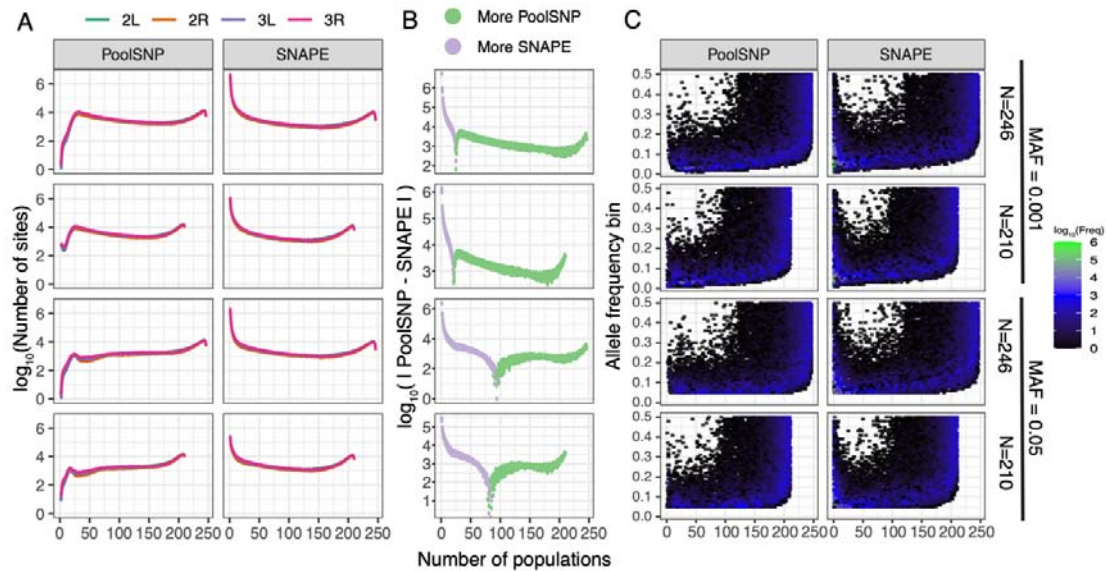
426

**Figure 2.** The effect of heuristic minor allele count (MAC) and minor allele frequency (MAF) thresholds on  $p_N/p_S$  ratios in SNP data based on PoolSNP (A) and SNAPE-pooled (B). Blue lines in both panels show average genome-wide  $p_N/p_S$  ratios across 271 and 246 populations, respectively. The blue ribbons depict the corresponding standard deviations. The bottom panels (C) and (D), correspond to the top panels A and B but excluding 36 problematic samples, which are characterized by elevated  $p_N/p_S$ , an exceptionally large number of private SNPs and genome-wide positive Tajima's  $D$ . Note that the y-axes of the bottom and top panels differ in scale. The two arrows show the MAC and MAF thresholds used for the final datasets.

434

436 **Patterns of polymorphism between PoolSNP and SNAPE-pooled.** We calculated three  
metrics related to the amount of polymorphism discovered by our pipelines: the abundance  
438 of polymorphisms segregating in  $n$  populations across each chromosome (Figure 3A), the  
difference of discovered polymorphisms between SNAPE-pooled and PoolSNP (defined as  
440 the absolute value of PoolSNP minus SNAPE-pooled; Figure 3B), and the amount of  
polymorphism discovered per minor allele frequency bin (Figure 3C). We evaluated these  
442 three metrics across a 2x2 filtering scheme: two MAF filters (0.001, 0.05) and two sample  
sets (the whole dataset of 246 samples; and the 210 samples that passed the sequencing  
444 error filter in SNAPE-pooled; see *Identification and quality control*). Notably, PoolSNP was  
biased towards identification of common SNPs present in multiple samples, whereas  
446 SNAPE-pooled was more sensitive to the identification of polymorphisms that appeared in  
few populations only (Figure 3B). For example, at a MAF filter of 0.001, SNAPE-pooled  
448 discovered more polymorphisms that were shared in less than 25 populations (relative to  
PoolSNP), and these accounted for ~79% of all polymorphisms discovered by the pipeline.  
450 Likewise, at a MAF filter of 0.05, SNAPE-pooled discovered more polymorphisms that were  
shared in less than 97 populations; these accounted for ~71% of all discovered  
452 polymorphisms. SNAPE-pooled identifies fewer polymorphic sites that are shared among a  
large number of populations than PoolSNP does because SNAPE pooled does not integrate  
454 information across multiple populations. As a consequence, it can fail to identify SNPs which  
are overall at low frequencies and get called as monomorphic or missing in a subset of  
456 populations given the posterior-probability thresholds that we employed (see Materials and  
Methods).

458 We also compared allele frequency estimates between the two callers using the  
aforementioned dataset of 210 populations applying a MAF filter of 0.05 (see Supplemental  
460 Material, Table S2). Among the positions identified as polymorphic by both calling methods,  
our frequency estimates were consistent for the great majority of SNPs in all samples  
462 analyzed (> 97% of samples). A very small proportion differed in less than 5% frequency  
among both methods (< 2.3% in all samples), and very few polymorphic SNPs differed by a  
464 frequency of between 5-10% (< 0.15% in all samples) or greater than 10% (< 0.03% in all  
samples) (Supplemental Material, Table S4). Positions with a discordant calling represented  
466 less than a 25% of all common positions in all samples (Supplemental Material, Table S4),  
the majority of them being called polymorphic by PoolSNP and classified as missing data by  
468 SNAPE-pooled (Supplemental Material, Table S4). This is consistent with the SNAPE-  
pooled method as well as the stringent parameters used (see Materials and Methods).



470

472

474

476

478

480

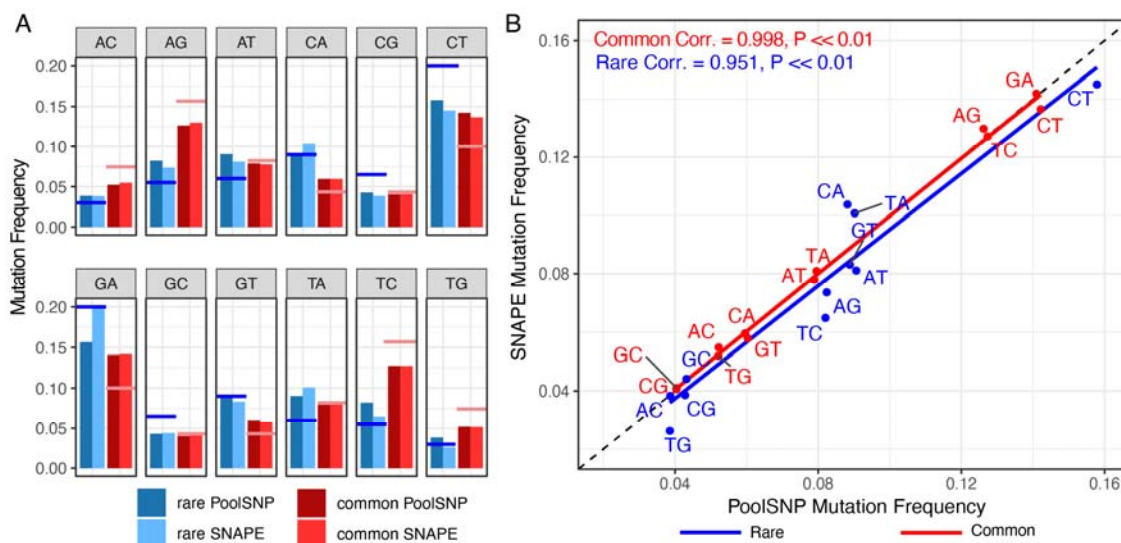
**Figure 3.** (A) Number of polymorphic sites discovered across populations. The x-axis shows the number of populations which share a polymorphic site. The y-axis corresponds to the number of polymorphic sites shared by any number of populations, on a log<sub>10</sub> scale. The colored lines represent different chromosomes, and are stacked on top of each other. (B) The difference of discovered polymorphisms between SNAPE-pooled and PoolSNP. (C) Number of polymorphic sites as a function of allele frequency and the number of populations the polymorphisms is present in. The color gradient represents the number of variant alleles from low to high (black to green). The x-axis is the same as in A, and the y-axis is the minor allele frequency. The 2x2 filtering scheme is shown on the right side of the figure.

**Mutation-class frequencies.** We estimated the percentage of mutation classes (e.g., A→C, A→G, A→T, etc.) accepted as polymorphisms in both our SNP calling pipelines, and classified these loci as being either “rare” (i.e., allele frequency < 5% and shared in less than 50 populations) or “common” (allele frequency > 5% and shared in more than 150 populations). For this analysis, we classified the minor allele as the derived allele. Figure 4A shows the percentage of each mutation class for the 210 populations which passed filters in both SNAPE-pooled and PoolSNP. In addition, we overlaid, as a horizontal line, the expected mutation frequencies for rare (blue; Assaf *et al.* 2017) and common (red; Mackay *et al.* 2012) mutations. For example, A→C variants are expected to be more abundant as common mutations than as rare mutations, and the opposite is true for C→A variants. In general, our SNP discovery pipelines produced mutation-class relative frequencies of rare and common mutations that are consistent with empirical expectations, however, there were some exceptions to this pattern. For example, the frequencies of the C/G rare mutation-class was consistently underestimated by both callers, a phenomenon that might be related to the known GC bias of modern sequencing machines (Benjamini and Speed 2012). The

494

496 correlation between SNP calling pipelines was high across both common and rare mutation  
 498 classes, with marginal discrepancies observed for rare variants (Figure 4B).

498



500 **Figure 4.** Frequencies of observed nucleotide polymorphism in the DEST dataset (210 populations  
 502 common to PoolSNP and SNAPE-pooled). (A) Each panel represents a mutation type. The red color  
 504 indicates common mutations (AF > 0.05, and common in more than 150 populations) whereas the  
 506 blue color indicates rare mutations (AF < 0.05, and shared in less than 50 populations). The dark  
 508 colors correspond to the PoolSNP pipeline and the soft colors correspond to the SNAPE-pooled  
 pipeline. The hovering red and blue horizontal lines represent the estimated mutation rates for  
 common and rare mutations, respectively. (B) Correlation between the observed mutation frequencies  
 seen in SNAPE-pooled and PoolSNP. The one-to-one correspondence line is shown as a black-  
 dashed diagonal. Correlation estimates (Pearson's correlation) and *p*-values for common and rare  
 mutations are shown.

510

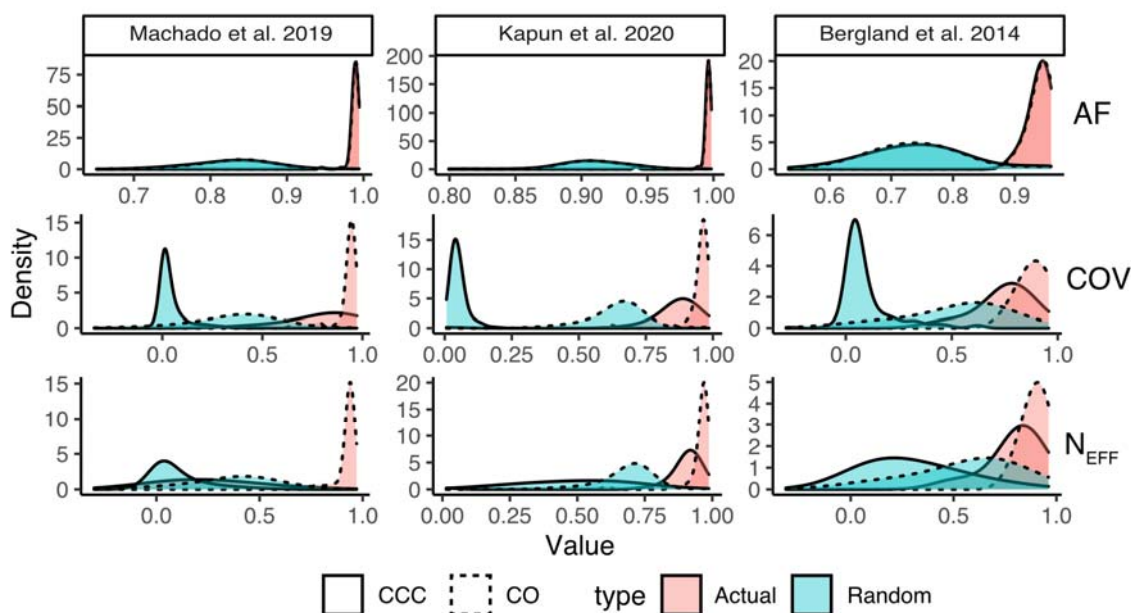
**Comparison to previously published datasets.** We compared the allele frequency and  
 512 read depth estimates from the DEST dataset (based on PoolSNP) to previously published  
 estimates by Bergland *et al.* (2014), Machado *et al.* (2019), and Kapun *et al.* (2020). For  
 514 these datasets we employed two types of correlations, the nominal correlation (i.e.,  
 Pearson's correlation; CO) and the concordance correlation coefficient (CCC; Lin 1989; Liao  
 516 and Lewis 2000). The CCC determines how much the observed data deviate from the line of  
 perfect concordance (i.e., the 45 degree-line on a square scatter plot).

518 Estimates of allele frequency were strongly correlated and consistent with previously  
 published data. The strongest correlation of DEST allele frequencies and previously  
 520 published allele frequencies was observed with the data of Kapun *et al.* (2020) (average CO  
 and CCC > 0.99; Figure 5, top row; Supplemental Material, Figure S4). Allele frequency  
 522 correlations with Machado *et al.* (2019) are also generally high (average CO and CCC >

0.98; Figure 5, top row; Supplemental Material, Figure S5). Allele frequency correlations with  
524 the data from Bergland *et al.* (2014) were lower (0.94; Supplemental Material, Figure S6),  
likely reflecting differences in data processing and quality control.

526 We also examined two aspects of read depth, i.e., nominal coverage and effective  
coverage. Nominal coverage is the number of reads mapping to a site that has passed  
528 quality control. Effective coverage is the approximate number of independent reads, after  
accounting for double binomial sampling, and is useful for obtaining unbiased estimates of  
530 the precision of allele frequency estimates (Kolaczkowski *et al.* 2011; Kofler *et al.* 2011a;  
Feder *et al.* 2012; Schlötterer *et al.* 2014). Similar to allele frequency estimates, the Pearson  
532 correlation coefficients for both coverage and effective coverage were large (0.92, 0.95, 0.90  
for Machado *et al.* (2019), Kapun *et al.* (2020), and Bergland *et al.* (2014), respectively; see  
534 Supplemental Material, Figures S7-12), indicating that sample identity was preserved  
appropriately. However, the concordance correlation coefficients were substantially lower  
536 between the datasets (0.24, 0.88, 0.79, respectively), indicating systematic differences in  
read depth between the DEST dataset and previously published data. Indeed, read depth  
538 estimates were on average ~12%, ~14% and ~20% lower in the DEST dataset as compared  
to the previously published data in Machado *et al.* (2019), Kapun *et al.* (2020), and Bergland  
540 *et al.* (2014)(2014) respectively. The lower read depth and effective read depth estimates in  
the DEST dataset reflects our more stringent quality control and filtering.

542



544

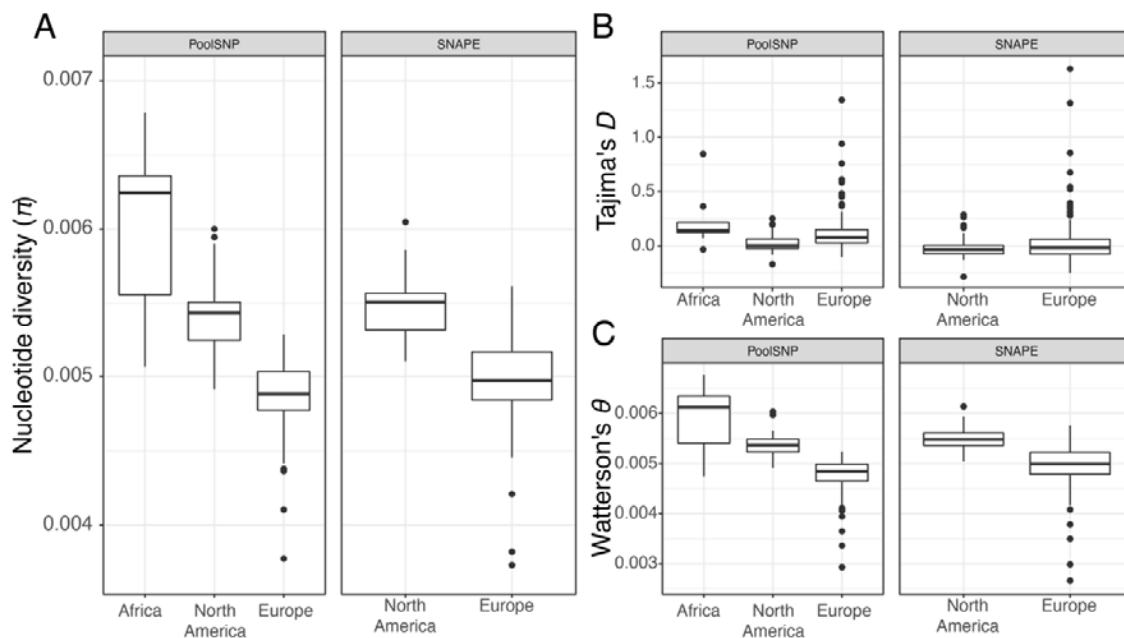
**Figure 5. Correlations between DEST dataset and previously published datasets.** Correlations  
546 between allele frequencies (AF), Nominal Coverage (COV), and Effective Coverage (N<sub>EFF</sub>) between



the DEST dataset (using the PoolSNP method) and three previously *Drosophila* datasets: Machado *et al.* (2019), Kapun *et al.* (2020), and Bergland *et al.* (2014). For each dataset, we show the distribution of two types of correlation coefficients: the nominal (Pearson's) correlation (CO; dashed lines) and the concordant correlation (CCC; solid lines). In addition to the actual correlations between the datasets (red distributions), we show the distributions of correlations estimated with random population pairs (green distributions).

**Genetic diversity.** We estimated nucleotide diversity ( $\pi$ ), Watterson's  $\theta$  and Tajima's  $D$  for both the PoolSNP and SNAPE-pooled datasets (Supplemental Material, Table S5). Results for the African, European and North American population samples are presented in Figure 6 (also see Supplemental Material, Figure S13 for estimates by chromosome arm). All estimates were positively correlated between PoolSNP and SNAPE-pooled ( $p < 0.001$ ), with Pearson's correlation coefficients of 0.88, 0.94 and 0.73 for  $\pi$ , Watterson's  $\theta$ , and Tajima's  $D$ , respectively. Higher values of genetic diversity were obtained for the SNAPE-pooled dataset, probably due to its higher sensitivity for detecting rare variants (see *Patterns of polymorphism between PoolSNP and SNAPE-pooled*). Pool size had no significant effect on the four summary statistics in European or in North American populations (GLMs, all  $p > 0.05$ ), suggesting that data from populations with heterogeneous pool sizes can be safely merged for accurate population genomic analysis.

566



568 **Figure 6.** Population genetic estimates for African, European and North American populations. Shown are genome-wide estimates of (A) nucleotide diversity ( $\pi$ ), (B) Watterson's  $\theta$  and (C) Tajima's  $D$  for African populations using the PoolSNP data set, and for European and North American populations using both the PoolSNP and SNAPE-pooled (SNAPE) datasets. As can be seen from the

570

572 figure, estimates based on PoolSNP versus SNAPE-pooled (SNAPE) are highly correlated (see main  
574 text). Genetic variability is seen to be highest for African populations, followed by North American and  
then European populations, as previously observed (e.g., see Lack *et al.* 2016; Kapun *et al.* 2020).

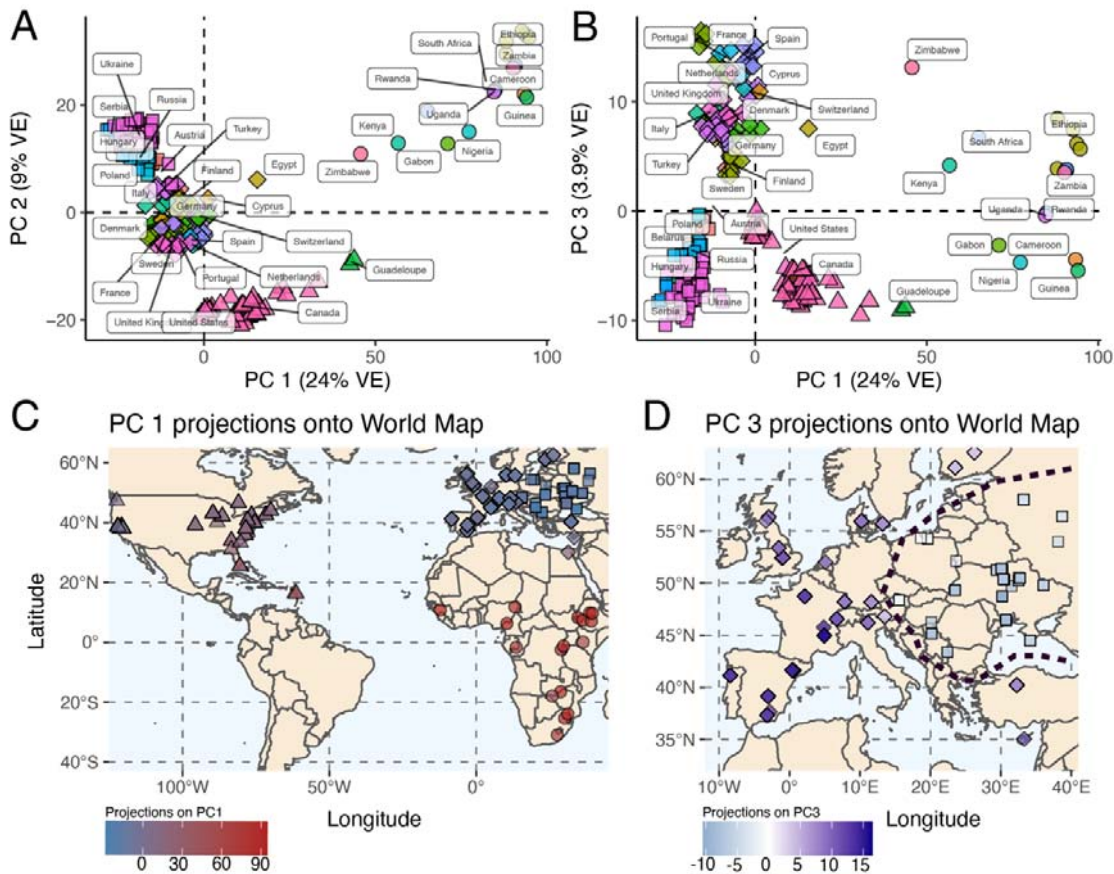
576 The highest levels of genetic variability were observed for ancestral African populations  
(mean  $\pi = 0.0060$ , mean  $\theta = 0.0059$ ); North American populations exhibited higher genetic  
578 variability (mean  $\pi = 0.0054$ , mean  $\theta = 0.0054$ ) than European populations (mean  $\pi =$   
0.0049, mean  $\theta = 0.0048$ ). These results are consistent with previous observations based on  
580 individual genome sequencing (e.g., see Lack *et al.* 2016; Kapun *et al.* 2020). Our  
observations are also consistent with previous estimates based on pooled data from three  
582 North American populations (mean  $\pi = 0.00577$ , mean  $\theta = 0.00597$ ; Fabian *et al.* 2012) and  
48 European populations (mean  $\pi = 0.0051$ , mean  $\theta = 0.0052$ ; Kapun *et al.* 2020).  
584 Estimates of Tajima's  $D$  were positive when using PoolSNP, and slightly negative using  
SNAPE. These results are expected given biases in the detection of rare alleles between  
586 these two SNP calling methods. In addition, our estimates for  $\pi$ , Watterson's  $\theta$  and Tajima's  
 $D$  were positively correlated with previous estimates for the 48 European populations  
588 analyzed by Kapun *et al.* (2020) (all  $p < 0.01$ ). Notably, slightly lower levels of Tajima's  $D$  in  
North America compared to both Africa and Europe (Figure 6B) may be indicative for  
590 admixture (Stajich and Hahn 2005) which has been identified previously along the North  
American east coast (Caracristi and Schlötterer 2003; Kao *et al.* 2015; Bergland *et al.* 2016).

592

**Phylogeographic clusters in *D. melanogaster*.** We performed PCA on the PoolSNP  
594 variants in order to include samples from North America (DrosRTEC), Europe (DrosEU), and  
Africa (DGN) datasets (excluding all Asian and Oceanian samples). Prior to analysis we  
596 filtered the joint datasets to include only high-quality biallelic SNPs. Because LD decays  
rapidly in *Drosophila* (Comeron *et al.* 2012), we only considered SNPs at least 500 bp away  
598 from each other. PCA on the resulting 100,000 SNPs revealed evidence for discrete  
phylogeographic clusters that correspond to geographic regions (Supplemental Material,  
600 Figure S14B). PC1 (24% variance explained [VE]) partitions samples between Africa and the  
other continents (Figure 7A). PC2 (9% VE) separates European from North American  
602 populations, and both PC2 and PC3 (4% VE) divide Europe into two population clusters  
(Figure 7B). Notably, these spatial relationships become evident when PCA projections from  
604 each sample are plotted onto a world map (Figure 7C). Interestingly, the emergent clusters  
in Europe are not strictly defined by geography. For example, the western cluster (diamonds  
606 in Figure 7D) includes Western Europe as well as Finland, Turkey, Cyprus, and Egypt. The  
eastern cluster, on the other hand, consists of several populations collected in previous  
608 Soviet republics as well as Poland, Hungary, Serbia and Austria, raising the possibility that



610 recent geo-political division in Europe could have affected migration and population  
611 structure. Whether this result arises as a relic of recent geopolitical history within Europe,  
612 more ancient migration and colonization (e.g., following post-glacial range expansion, Kapun  
*et al.* 2020), local adaptation, or sampling strategy (Novembre and Stephens 2008; cf.  
613 Kapun *et al.* 2020) remains unknown. Future targeted sampling is needed to resolve these  
614 alternative explanations.



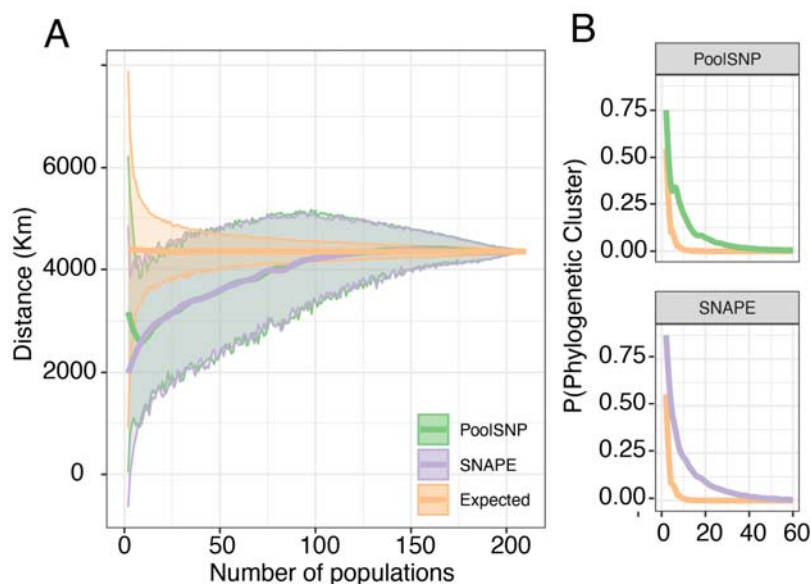
616

618 **Figure 7.** Demographic signatures of the DrosEU, DrosRTEC, and DGN data (using the PoolSNP  
619 pipeline). (A) PCA dimensions 1 and 2. The mean centroid of a country's assignment is labeled. (B)  
620 PCA dimensions 1 and 3. (C) Projections of PC1 onto a World map. PC1 projections define the  
621 existence of continental level clusters of population structure (indicated by the shapes circles: Africa;  
622 triangles: North America; diamonds and squares: Europe). (D) Projections of PC3 onto Europe. These  
623 projections show the existence of a demographic divide within Europe: the diamond shapes indicate a  
624 western cluster, whereas the squares represent an eastern cluster. For panels C and D, the intensity  
625 of the color is proportional to the PC projection. The black dashed line shows the two-cluster divide.

626

A unique feature of this dataset is that it contains a mixture of Pool-Seq and inbred (or haploid) genome data. For some geographic regions, the DEST dataset contains both data types. Inbred and Pool-Seq samples from nearby geographic regions clustered in the same regions of PC space (Supplemental Material, Figure S15). Excluding the DGN-derived African samples, no PC was significantly correlated with data type (PC1  $p = 0.352$ , PC2  $p = 0.223$ , PC3  $p = 0.998$ ).

**Geographic proximity analysis.** The geographic distribution of our samples allows leveraging basic principles of phylogeography and population genetics to assess the biological significance of rare SNPs (Wright 1943; Battey *et al.* 2020). Accordingly, we expect to observe young neutral alleles at low frequencies among geographically close populations. We tested this hypothesis by estimating the average geographic distance among pairs of populations that share SNPs only occurring in these two populations (doubletons), among three populations that share tripletons, and so forth. Without imposing a MAF filter, both SNAPE-pooled and PoolSNP pipelines produced patterns concordant with the expectation. Populations in close proximity were more likely to share rare mutations relative to random chance pairings (Figure 8A). Notably, the PoolSNP dataset showed an elevated number of rare alleles, which violate the phylogeographic expectation (Figure 8A); however, this only affects 0.31% of all PoolSNP mutations. To further evaluate this pattern, we estimated the probability that any given population pair belongs to a particular phylogeographic cluster (Supplemental Material, Figure S16) as a function of their shared variants. Our results indicate that rare variants, private to geographically proximate populations, are strong predictors of phylogeographic provenance (see Figure 8B).



650

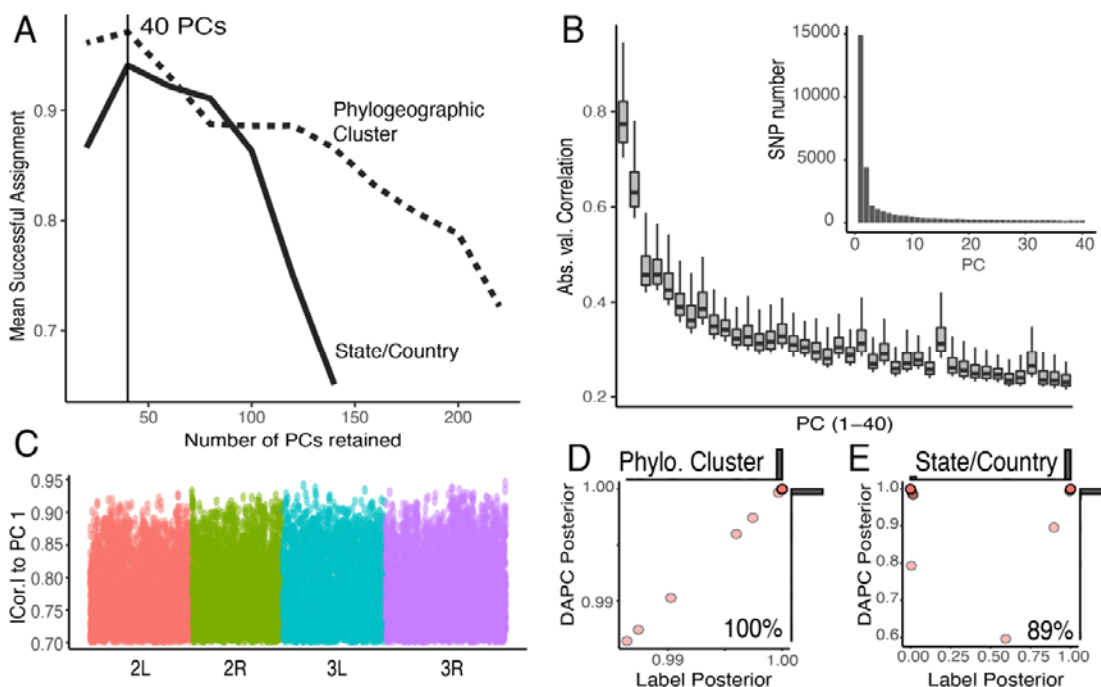
**Figure 8.** Geographic Proximity Analysis. (A) Average geographic distance between populations that share a polymorphism at any given site for PoolSNP and SNAPE-pooled. The x-axis represents the number of populations considered; the y-axis is the mean geographic distance among samples. The yellow line represents the random expectation calculated as random pairings of the data. The band around the lines is the standard deviation of the estimator. (B) Probability that all populations containing a polymorphic site come from the same phylogeographic cluster (Supplemental Figure 14). The y-axis is the probability of “x” populations belonging to the same phylogeographic cluster. The axis only shows up to 40 populations; after that point, the probability approaches 0. The colors are consistent across panels.

660

**Demography-informative markers.** An inherent strength of our broad biogeographic sampling is the potential to generate a panel of core demography SNPs to investigate the provenance of current and future samples. We created a panel of demography-informative markers (DIMs) by conducting a DAPC to discover which loci drive the phylogeographic signal in the dataset. We trained two separate DAPC models: the first utilized the four phylogeographic clusters identified by principal components (PCs; Figure 6AB, Supplemental Material, Figure S16, Table S1); the second utilized the geographic localities where the samples were collected (i.e., countries in Europe and the US states). This optimization indicated that the information contained in the first 40 PCs maximizes the probability of successful assignment (Figure 9A). This resulted in the inclusion of 30,000 DIMs, most of which were strongly associated with PCs 1-3 (Figure 9B inset). Moreover, the correlations were larger among the first 3 PCs and decayed monotonically for the additional PCs (Figure 9B). Lastly, our DIMs were uniformly distributed across the fly genome (Figure 9C).

We assessed the accuracy of our DIM panel using a leave-one-out cross-validation approach (LOOCV). We trained the DAPC model using all but one sample and then classified the excluded sample. We performed LOOCV separately for the phylogeographic cluster groups, as well as for the state/country labels. The phylogeographic model used all DrosRTEC, DrosEU, and DGN samples (excluding Asia and Oceania with too few individuals per sample); the state/country model used only samples for which each label had at least 3 or more samples. Our results showed that the model is 100% accurate in terms of resolving samples at the phylogeographic cluster level (Figure 9D) and 89% at the state/country level (Figure 9E). We anticipate that this set of DIMs will be useful for future analysis of geographic provenance of North American and European samples. We provide a tutorial on the usage of the DIM in Supplemental Methods.

686



688 **Figure 9.** Demography-informative markers. (A) Number of retained PCs which maximize the DAPC  
 690 model's capacity to assign group membership. Model trained on the phylogeographic clusters  
 692 (dashed lines) or the country/state labels (solid line). (B) Absolute correlation for the 33,000 individual  
 694 SNPs with highest weights onto the first 40 components of the PCA. Inset: Number of SNPs per PC.  
 696 (C) Location of the 33,000 most informative demographic SNPs across the chromosomes. (D)  
 LOOCV of the DAPC model trained on the phylogeographic clusters. (E) LOOCV of the DAPC model  
 trained on the phylogeographic state/country labels. For panels D and E, the y-axis shows the highest  
 posterior produced by the prediction model and the x-axis is the posterior assigned to the actual label  
 classification of the sample. Also, for D and E, marginal histograms are shown.

698

## Conclusions and Outlook

Here we have presented a new, modular and unified bioinformatics pipeline for processing,  
 700 integrating and analyzing SNP variants segregating in population samples of *D.*  
*melanogaster*. We have used this pipeline to assemble the largest worldwide data repository  
 702 of genome-wide SNPs in *D. melanogaster* to date, based both on previously published data  
 (DGN: Africa; Lack *et al.* 2015, 2016) as well as on new data collected by our two  
 704 collaborating consortia (DrosRTEC: mostly North America; Machado *et al.* 2019; DrosEU:  
 mostly Europe; Kapun *et al.* 2020). We assembled this dataset using two SNP calling  
 706 strategies that differ in their ability to identify rare polymorphisms, thereby enabling future  
 work studying the evolutionary history of this species. We are dubbing this data repository  
 708 and the supporting bioinformatics tools *Drosophila Evolution over Space and Time* (DEST).

One of the biggest challenges in the present “omics” era is the rapidly growing number  
710 of complex large-scale datasets which require technically elaborate bioinformatics know-how  
to become accessible and utilizable. This hurdle often prohibits the exploitation of already  
712 available genomics datasets by scientists without a strong bioinformatics or computational  
background. To remedy this situation for the *Drosophila* evolution community, our  
714 bioinformatics pipeline is provided as a Docker image (to standardize across software  
versions, as well as make the pipeline independent of specific operating systems) and a new  
716 genome browser makes our SNP dataset available through an easy-to-use web interface  
(see Supplemental Information Figures S2, S3; available at <https://dest.bio>).

718 The DEST data repository and platform will enable the population genomics community  
to address a variety of longstanding, fundamental questions in ecological and evolutionary  
720 genetics. The current dataset might for instance be valuable for providing a more accurate  
picture of the demographic history of *D. melanogaster* populations, in particular in Europe  
722 and North America, and with respect to multiple bouts of out-of-Africa migration and recent  
patterns of admixture.

724 The DEST dataset will likewise be useful for an improved understanding of the genomic  
signatures underlying both global and local adaptation, including a more fine-grained view of  
726 selective sweeps, their evolutionary origin and distribution (e.g., see Glinka *et al.* 2003;  
Beisswanger *et al.* 2006; Ometto 2010; Stephan 2016; Kapun *et al.* 2020). In terms of local  
728 adaptation, the broad spatial sampling across latitudinal and longitudinal gradients on the  
North American and European continents, encompassing a broad range of climate zones  
730 and areas of varying degrees of seasonality, will allow examining the parallel nature of local  
(clinal) adaptation in response to similar environmental factors in greater depth than possible  
732 before (e.g., Turner *et al.* 2008; Kolaczkowski *et al.* 2011; Fabian *et al.* 2012; Reinhardt *et al.*  
2014; Kapun *et al.* 2016, 2020; Machado *et al.* 2019; Bogaerts-Márquez *et al.* 2020;  
734 Waldvogel *et al.* 2020).

Another major opportunity provided by the DEST dataset lies in studying the temporal  
736 dynamics of evolutionary change. Sampling at dozens of localities across the growing  
season and over multiple years will help to advance our understanding of the short-term  
738 population and evolutionary dynamics of flies living in diverse environments, thereby  
providing novel insights into the nature of temporally varying selection (e.g., Wittmann *et al.*;  
740 Bergland *et al.* 2014; Machado *et al.* 2019) and evolutionary responses to climate change  
(e.g., Umina 2005; Rodríguez-Trelles *et al.* 2013; Waldvogel *et al.* 2020).

742 Moreover, by integrating these worldwide estimates of allele frequencies, those from  
lab- and field-based ‘evolve and resequence’ (E&R; Turner *et al.* 2011; reviewed in Kofler  
744 and Schlötterer 2014; Schlötterer *et al.* 2014; Flatt 2020) and mesocosm experiments (e.g.,



Rudman *et al.* 2019; Erickson *et al.* 2020), we might be able to gain deeper insights into the genetic basis and evolutionary history of variation in fitness components (e.g., Flatt 2020).

The real value of the DEST dataset lies in the future: its long-term utility will grow as natural and experimental populations are continually being sampled, resequenced and added to the repository by the community of *Drosophila* evolutionary geneticists. The pipeline that we have established will make future updates to the data-repository straightforward. Furthermore, since it is not easily feasible for any single research group to sample flies densely through time and across a broad geographic range, the growing value of the DEST dataset will depend upon the synergistic collaboration among research groups across the globe, as exemplified by the DrosRTEC and DrosEU consortia. Importantly, in an era of rapidly decreasing sequencing costs, comprehensive population genomic analyses are no longer limited by genetic marker density but by the availability of biological samples from standardized, collaborative long-term collection efforts through space and time (e.g., Machado *et al.* 2019; Kapun *et al.* 2020). In this vein, the collaborative framework presented here might allow us, as a global community, to fill some important gaps in the current data repository: for example, many areas of the world (notably Asia and South America) remain largely uncharted territory in *Drosophila* population genomics, and the addition of phased sequencing data (e.g., providing information on haplotypes, LD, linked selection) will be crucially important for future analyses of demography, selection and their interplay.

We are convinced that the DEST platform will become a valuable and widely-used resource for scientists interested in *Drosophila* evolution and genetics, and we actively encourage the community to join the collaborative effort we are seeking to build.

## Data availability

All scripts to make figures and perform analyses associated with this manuscript are available here: <https://github.com/DEST-bio/data-paper>. All scripts to build the dataset, including the mapping pipeline, SNP calling scripts, and meta-data are available here: [https://github.com/DEST-bio/DEST\\_freeze1](https://github.com/DEST-bio/DEST_freeze1). All output from the DEST pipeline, including intermediate output files, metadata, etc. can be found here: <https://dest.bio>. The genome browser associated with the DEST dataset can be found here: <http://dgvbrowser.uab.cat/dest/browser/>. The mapping and SNP calling pipeline can be found here: <https://hub.docker.com/r/destbiodocker/destbiodocker>

## Acknowledgements

We are grateful to all the members of the DrosEU and DrosRTEC consortia for their long-standing support, collaboration and for discussion. DrosEU is funded by a Special Topic

782 Networks (STN) grant from the European Society for Evolutionary Biology (ESEB). MK (M.  
784 Kapun) was supported by the Austrian Science Foundation (grant no. FWF P32275); JG by  
786 the European Research Council (ERC) under the European Union's Horizon 2020 research  
788 and innovation programme (H2020-ERC-2014-CoG-647900) and by the Spanish Ministry of  
790 Science and Innovation (BFU-2011-24397); TF by the Swiss National Science Foundation  
792 (SNSF grants PP00P3\_133641, PP00P3\_165836, and 31003A\_182262) and a Mercator  
794 Fellowship from the German Research Foundation (DFG), held as a EvoPAD Visiting  
796 Professor at the Institute for Evolution and Biodiversity, University of Münster; AOB by the  
798 National Institutes of Health (R35 GM119686); MK (M. Kankare) by Academy of Finland  
grant 322980; VL by Danish Natural Science Research Council (FNU) grant 4002-00113B;  
FS Deutsche Forschungsgemeinschaft (DFG) grant STA1154/4-1, Project 408908608; JP  
by the Deutsche Forschungsgemeinschaft Projects 274388701 and 347368302; AU by FPI  
fellowship (BES-2012-052999); ET Israel Science Foundation (ISF) grant 1737/17; MSV,  
MSR and MJ by a grant from the Ministry of Education, Science and Technological  
Development of the Republic of Serbia (451-03-68/2020-14/200178); AP, KE and MT by a  
grant from the Ministry of Education, Science and Technological Development of the  
Republic of Serbia (451-03-68/2020-14/200007); and TM NSERC grant RGPIN-2018-05551.

### Author contributions

800 Martin Kapun: Conceptualization, Data curation, Formal Analysis, Funding acquisition,  
802 Investigation, Methodology, Project Administration, Resources, Software, Supervision,  
804 Visualization, Writing - original draft, Writing - review & editing. Joaquin Nunez: Formal  
806 Analysis, Methodology, Software, Visualization, Writing - original draft, Writing - review &  
808 editing. María Bogaerts-Márquez: Formal Analysis, Methodology, Software, Visualization,  
810 Writing - original draft, Writing - review & editing. Jesús Murga-Moreno: Formal Analysis,  
812 Methodology, Software, Visualization, Writing - original draft, Writing - review & editing.  
814 Margot Paris: Formal Analysis, Methodology, Software, Visualization, Writing - original draft,  
816 Writing - review & editing. Joseph Outten: Software, Writing - review & editing. Marta  
Coronado-Zamora: Formal Analysis, Methodology, Software, Visualization, Writing - original  
draft, Writing - review & editing. Aleksandra Patenkovic: Resources. Amanda Glaser-  
Schmitt: Resources. Anna Ullastres: Resources. Antonio J. Buendía-Ruíz: Resources. Banu  
S. Onder: Resources. Brian P Lazzaro: Resources, Writing - review & editing. Catherine  
Montchamp-Moreau: Resources. Christopher W. Wheat: Resources, Writing - review &  
editing. Cristina P. Vieira: Resources, Writing - review & editing. Daniel K. Fabian:  
Resources. Darren J. Obbard: Resources. Dmitry V. Mukha: Resources. Dorcas J. Orengo:  
Resources, Writing - review & editing. Elena Pasyukova: Resources. Eliza Argyridou:



Resources. Emily L. Behrman: Resources, Writing - review & editing. Eran Tauber:  
818 Resources. Eva Puerma: Resources, Writing - review & editing. Fabian Staubach:  
Resources, Writing - review & editing. Francisco D Gallardo-Jiménez: Resources. Iryna  
820 Kozeretska: Resources. J. Roberto Torres: Resources. Jessica K. Abbott: Resources. John  
Parsch: Funding acquisition, Resources, Writing - review & editing. Jorge Vieira: Resources,  
822 Writing - review & editing. M. Josefa Gómez-Julián: Resources. Katarina Eric: Resources.  
Kelly A. Dyer: Resources. Lain Guio: Resources. Lino Ometto: Writing - review & editing. M.  
824 Luisa Espinosa-Jimenez: Resources. Maaria Kankare: Resources, Writing - review &  
editing. Mads F. Schou: Resources, Writing - review & editing. Maria P. García Guerreiro:  
826 Resources, Writing - review & editing. Marija Savic Veselinovic: Resources. Marija  
Tanaskovic: Resources. Marina Stamenkovic-Radak: Funding acquisition, Resources.  
828 Mihailo Jelic: Resources. Miriam Merenciano: Resources. Oleksandr M. Maistrenko: Writing  
- review & editing. Omar Rota-Stabelli: Resources. Sara Guirao-Rico: Resources, Writing -  
830 review & editing. Sònia Casillas: Resources, Writing - review & editing. Sonja Grath:  
Resources. Stephen W. Schaeffer: Resources. Subhash Rajpurohit: Resources. Svitlana V.  
832 Serga: Resources. Thomas J.S. Merritt: Resources. Vivien Horváth: Resources. Vladimir E.  
Alatortsev: Resources. Volker Loeschcke: Resources. Yun Wang: Resources. Antonio  
834 Barbadilla: Software, Writing - review & editing. Dmitri Petrov: Conceptualization, Funding  
acquisition, Project Administration, Resources, Writing - review & editing. Paul Schmidt:  
836 Conceptualization, Funding acquisition, Project Administration, Resources, Writing - review  
& editing. Josefa Gonzalez: Conceptualization, Funding acquisition, Project Administration,  
838 Resources, Supervision, Writing - original draft, Writing - review & editing. Thomas Flatt:  
Conceptualization, Funding acquisition, Project Administration, Resources, Supervision,  
840 Writing - original draft, Writing - review & editing. Alan Bergland: Conceptualization, Data  
curation, Formal Analysis, Funding acquisition, Investigation, Methodology, Project  
842 Administration, Resources, Software, Supervision, Visualization, Writing - original draft,  
Writing - review & editing

844

**Competing interests.** The authors declare no competing interests.

846

## References

- 848 Adams, M. D., 2000 The Genome Sequence of *Drosophila melanogaster*. *Science* 287:  
2185–2195.
- 850 Andrews, S., 2010 FastQC: A Quality Control Tool for High Throughput Sequence Data.  
Available online at: <http://www.bioinformatics.babraham.ac.uk/projects/fastqc/>

- 852 Arguello, J. R., S. Laurent, and A. G. Clark, 2019 Demographic History of the Human  
Commensal *Drosophila melanogaster*. *Genome Biol Evol* 11: 844–854.
- 854 Assaf, Z. J., S. Tilk, J. Park, M. L. Siegal, and D. A. Petrov, 2017 Deep sequencing of  
natural and experimental populations of *Drosophila melanogaster* reveals biases in  
856 the spectrum of new mutations. *Genome Res* 27: 1988–2000.
- Bastide, H., A. Betancourt, V. Nolte, R. Tobler, P. Stöbe *et al.*, 2013 A Genome-Wide, Fine-  
858 Scale Map of Natural Pigmentation Variation in *Drosophila melanogaster*. *PLoS  
Genet* 9: e1003534.
- 860 Battey, C. J., P. L. Ralph, and A. D. Kern, 2020 Space is the Place: Effects of Continuous  
Spatial Structure on Analysis of Population Genetic Data. *Genetics* 215: 193–214.
- 862 Behrman, E. L., V. M. Howick, M. Kapun, F. Staubach, A. O. Bergland *et al.*, 2018 Rapid  
seasonal evolution in innate immunity of wild *Drosophila melanogaster*. *Proc Royal  
864 Soc B* 285: 20172599.
- Beisswanger, S., W. Stephan, and D. Lorenzo, 2006 Evidence for a Selective Sweep in the  
866 *wapl* Region of *Drosophila melanogaster*. *Genetics* 172: 265–274.
- Benjamini, Y., and T. P. Speed, 2012 Summarizing and correcting the GC content bias in  
868 high-throughput sequencing. *Nucleic Acids Res* 40: e72.
- Bergland, A. O., E. L. Behrman, K. R. O'Brien, P. S. Schmidt, and D. A. Petrov, 2014  
870 Genomic Evidence of Rapid and Stable Adaptive Oscillations over Seasonal Time  
Scales in *Drosophila*. *PLoS Genet* 10: e1004775.
- 872 Bergland, A. O., R. Tobler, J. González, P. Schmidt, and D. Petrov, 2016 Secondary contact  
and local adaptation contribute to genome-wide patterns of clinal variation in  
874 *Drosophila melanogaster*. *Mol Ecol* 25: 1157–1174.
- Bogaerts-Márquez, M., S. Guirao-Rico, M. Gautier, and J. González, 2020 Temperature,  
876 rainfall and wind variables underlie environmental adaptation in natural populations  
of *Drosophila melanogaster*. *Mol Ecol*, in press (<https://doi.org/10.1111/mec.15783>).
- 878 Buels, R., E. Yao, C. M. Diesh, R. D. Hayes, M. Munoz-Torres *et al.*, 2016 JBrowse: a  
dynamic web platform for genome visualization and analysis. *Genome Biol* 17: 66.
- 880 Burke, M. K., 2012 How does adaptation sweep through the genome? Insights from long-  
term selection experiments. *Proc Royal Soc B* 279: 5029–5038.
- 882 Bushnell, B., J. Rood, and E. Singer, 2017 BBMerge – Accurate paired shotgun read  
merging via overlap. *PLoS ONE* 12: e0185056.
- 884 Campo, D., K. Lehmann, C. Fjeldsted, T. Souaiaia, J. Kao *et al.*, 2013 Whole-genome  
sequencing of two North American *Drosophila melanogaster* populations reveals  
886 genetic differentiation and positive selection. *Mol Ecol* 22: 5084–5097.
- Capy, P., and P. Gibert, 2004 *Drosophila melanogaster*, *Drosophila simulans*: so similar yet  
888 so different. *Genetica* 120(1-3): 5-16.

- 890 Caracristi, G., and C. Schlötterer, 2003 Genetic Differentiation Between American and  
European *Drosophila melanogaster* Populations Could Be Attributed to Admixture of  
African Alleles. *Mol Biol Evol* 20: 792–799.
- 892 Celniker, S. E., and G. M. Rubin, 2003 The *Drosophila melanogaster* genome. *Annu Rev*  
*Genomics Hum Genet* 4: 89–117.
- 894 Cheng, C., B. J. White, C. Kamdem, K. Mockaitis, C. Costantini *et al.*, 2012 Ecological  
Genomics of *Anopheles gambiae* Along a Latitudinal Cline: A Population-  
896 Resequencing Approach. *Genetics* 190: 1417–1432.
- Cingolani, P., A. Platts, L. Wang, M. Coon, T. Nguyen *et al.*, 2012 A program for annotating  
898 and predicting the effects of single nucleotide polymorphisms, SnpEff. *Fly* 6: 80–92.
- Comeron, J. M., R. Ratnappan, and S. Bailin, 2012 The Many Landscapes of Recombination  
900 in *Drosophila melanogaster*. *PLoS Genet* 8: e1002905.
- Corbett-Detig, R., and R. Nielsen, 2017 A Hidden Markov Model Approach for  
902 Simultaneously Estimating Local Ancestry and Admixture Time Using Next  
Generation Sequence Data in Samples of Arbitrary Ploidy. *PLoS Genet* 13:  
904 e1006529.
- Danecek, P., A. Auton, G. Abecasis, C. A. Albers, E. Banks *et al.*, 2011 The variant call  
906 format and VCFtools. *Bioinformatics* 27: 2156–2158.
- David, J. R., and P. Capy, 1988 Genetic variation of *Drosophila melanogaster* natural  
908 populations. *Trends Genet* 4: 106–111.
- Deitz, K. C., G. A. Athrey, M. Jawara, H. J. Overgaard, A. Matias *et al.*, 2016 Genome-Wide  
910 Divergence in the West-African Malaria Vector *Anopheles melas*. *G3* 6: 2867–2879.
- Duchen, P., D. Živković, S. Hutter, W. Stephan, and S. Laurent, 2013 Demographic  
912 Inference Reveals African and European Admixture in the North American  
*Drosophila melanogaster* Population. *Genetics* 193: 291–301.
- 914 Duffy, J. B., 2002 GAL4 system in *Drosophila*: a fly geneticist’s Swiss army knife. *Genesis*  
34: 1–15.
- 916 Durmaz, E., C. Benson, M. Kapun, P. Schmidt, and T. Flatt, 2018 An inversion supergene in  
*Drosophila* underpins latitudinal clines in survival traits. *J Evolution Biol* 31: 1354–  
918 1364.
- Durmaz, E., S. Rajpurohit, N. Betancourt, D. K. Fabian, M. Kapun *et al.*, 2019 A clinal  
920 polymorphism in the insulin signaling transcription factor *foxo* contributes to life-  
history adaptation in *Drosophila*. *Evolution* 73: 1774–1792.
- 922 Erickson, P. A., C. A. Weller, D. Y. Song, A. S. Bangerter, P. Schmidt *et al.*, 2020 Unique  
genetic signatures of local adaptation over space and time for diapause, an  
924 ecologically relevant complex trait, in *Drosophila melanogaster*. *PLoS Genet* 16:  
e1009110.

- 926 Fabian, D. K., M. Kapun, V. Nolte, R. Kofler, P. S. Schmidt *et al.*, 2012 Genome-wide  
patterns of latitudinal differentiation among populations of *Drosophila melanogaster*  
928 from North America. *Mol Ecol* 21: 4748–4769.
- Feder, A. F., D. A. Petrov, and A. O. Bergland, 2012 LDx: Estimation of Linkage  
930 Disequilibrium from High-Throughput Pooled Resequencing Data. *PLoS ONE* 7:  
e48588.
- 932 Ferretti, L., S. E. Ramos-Onsins, and M. Pérez-Enciso, 2013 Population genomics from pool  
sequencing. *Mol Ecol* 22: 5561–5576.
- 934 Flatt, T., 2016 Genomics of clinal variation in *Drosophila*: disentangling the interactions of  
selection and demography. *Mol Ecol* 25: 1023–1026.
- 936 Flatt, T., 2020 Life-History Evolution and the Genetics of Fitness Components in *Drosophila*  
*melanogaster*. *Genetics* 214: 3–48.
- 938 Gautier, M., J. Foucaud, K. Gharbi, T. Cézard, M. Galan *et al.*, 2013 Estimation of population  
allele frequencies from next-generation sequencing data: pool-versus individual-  
940 based genotyping. *Mol Ecol* 22: 3766–3779.
- Giesen, A., W. U. Blanckenhorn, M. A. Schäfer, K. K. Shimizu, R. Shimizu-Inatsugi *et al.*,  
942 2020 Genomic signals of admixture and reinforcement between two closely related  
species of European sepsid flies. Preprint: bioRxiv 2020.03.11.985903.
- 944 Glinka, S., L. Ometto, S. Mousset, W. Stephan, and D. Lorenzo, 2003 Demography and  
natural selection have shaped genetic variation in *Drosophila melanogaster*: a multi-  
946 locus approach. *Genetics* 165: 1269–1278.
- Gould, B. A., Y. Chen, and D. B. Lowry, 2017 Pooled Ecotype Sequencing Reveals  
948 Candidate Genetic Mechanisms for Adaptive Differentiation and Reproductive  
Isolation. *Mol Ecol* 26: 163–177.
- 950 Grenier, J. K., J. R. Arguello, M. C. Moreira, S. Gottipati, J. Mohammed *et al.*, 2015 Global  
Diversity Lines—A Five-Continent Reference Panel of Sequenced *Drosophila*  
952 *melanogaster* Strains. *G3* 5: 593–603.
- Guirao-Rico, S., and J. González, 2021 Benchmarking the performance of Pool-seq SNP  
954 callers using simulated and real sequencing data. *Mol Ecol Res*, in press.
- Guirao-Rico, S., and J. González, 2019 Evolutionary insights from large scale resequencing  
956 datasets in *Drosophila melanogaster*. *Curr Opin Insect Sci* 31: 70–76.
- Hales, K. G., C. A. Korey, A. M. Larracuente, and D. M. Roberts, 2015 Genetics on the Fly:  
958 A Primer on the *Drosophila* Model System. *Genetics* 201: 815–842.
- Haudry, A., S. Laurent, and M. Kapun, 2020 Population genomics on the fly: recent  
960 advances in *Drosophila*. *Methods Mol Biol* 290: 357–396.

- Hijmans, R. J., S. E. Cameron, J. L. Parra, P. G. Jones, and A. Jarvis, 2005 Very high resolution interpolated climate surfaces for global land areas. *Int J Climatol* 25: 1965–1978.
- Hivert, V., R. Leblois, E. J. Petit, M. Gautier, and R. Vitalis, 2018 Measuring Genetic Differentiation from Pool-seq Data. *Genetics* 210: 315–330.
- Hoban, S., J. L. Kelley, K. E. Lotterhos, M. F. Antolin, G. Bradburd *et al.*, 2016 Finding the Genomic Basis of Local Adaptation: Pitfalls, Practical Solutions, and Future Directions. *Am Nat* 188: 379–397.
- Hu, T. T., M. B. Eisen, K. R. Thornton, and P. Andolfatto, 2013 A second-generation assembly of the *Drosophila simulans* genome provides new insights into patterns of lineage-specific divergence. *Genome Res* 23: 89–98.
- Jennings, B. H., 2011 *Drosophila* – a versatile model in biology & medicine. *Materials Today* 14: 190–195.
- Jombart, T., S. Devillard, and F. Balloux, 2010 Discriminant analysis of principal components: a new method for the analysis of genetically structured populations. *BMC Genetics* 11: 94.
- de Jong, G., and Z. Bochdanovits, 2003 Latitudinal clines in *Drosophila melanogaster*: Body size, allozyme frequencies, inversion frequencies, and the insulin-signalling pathway. *J Genet* 82: 207–223.
- Kao, J. Y., A. Zubair, M. P. Salomon, S. V. Nuzhdin, and D. Campo, 2015 Population genomic analysis uncovers African and European admixture in *Drosophila melanogaster* populations from the south-eastern United States and Caribbean Islands. *Mol Ecol* 24: 1499–1509.
- Kapopoulou, A., M. Kapun, B. Pieper, P. Pavlidis, R. Wilches *et al.*, 2020 Demographic analyses of a new sample of haploid genomes from a Swedish population of *Drosophila melanogaster*. *Sci Rep* 10: 22415.
- Kapun, M., M. G. Barrón, F. Staubach, D. J. Obbard, R. A. W. Wiberg *et al.*, 2020 Genomic Analysis of European *Drosophila melanogaster* Populations Reveals Longitudinal Structure, Continent-Wide Selection, and Previously Unknown DNA Viruses. *Mol Biol Evol* 37: 2661–2678.
- Kapun, M., D. K. Fabian, J. Goudet, and T. Flatt, 2016 Genomic Evidence for Adaptive Inversion Clines in *Drosophila melanogaster*. *Mol Biol Evol* 33: 1317–1336.
- Keller, A., 2007 *Drosophila melanogaster's* history as a human commensal. *Curr Biol* 17: R77–R81.
- Kent, W. J., A. S. Zweig, G. Barber, A. S. Hinrichs, and D. Karolchik, 2010 BigWig and BigBed: enabling browsing of large distributed datasets. *Bioinformatics* 26: 2204–2207.

- 998 Koboldt, D. C., K. Chen, T. Wylie, D. E. Larson, M. D. McLellan *et al.*, 2009 VarScan: variant  
detection in massively parallel sequencing of individual and pooled samples.  
1000 Bioinformatics 25: 2283–2285.
- Koboldt, D. C., Q. Zhang, D. E. Larson, D. Shen, M. D. McLellan *et al.*, 2012 VarScan 2:  
1002 Somatic mutation and copy number alteration discovery in cancer by exome  
sequencing. Genome Res 22: 568–576.
- 1004 Kofler, R., P. Orozco-terWengel, N. De Maio, R. V. Pandey, V. Nolte *et al.*, 2011a  
PoPoolation: A Toolbox for Population Genetic Analysis of Next Generation  
1006 Sequencing Data from Pooled Individuals. PLoS ONE 6: e15925.
- Kofler, R., R. V. Pandey, and C. Schlotterer, 2011b PoPoolation2: identifying differentiation  
1008 between populations using sequencing of pooled DNA samples (Pool-Seq).  
Bioinformatics 27: 3435–3436.
- 1010 Kofler, R., and C. Schlotterer, 2014 A guide for the design of evolve and resequencing  
studies. Mol Biol Evol 31: 474–483.
- 1012 Kolaczkowski, B., A. D. Kern, A. K. Holloway, and D. J. Begun, 2011 Genomic Differentiation  
Between Temperate and Tropical Australian Populations of *Drosophila*  
1014 *melanogaster*. Genetics 187: 245–260.
- Kuhn, R. M., D. Haussler, and W. J. Kent, 2013 The UCSC genome browser and associated  
1016 tools. Brief Bioinform 14: 144–161.
- Lachaise, D., M.-L. Cariou, J. R. David, F. Lemeunier, L. Tsacas *et al.*, 1988 Historical  
1018 Biogeography of the *Drosophila melanogaster* Species Subgroup, pp. 159–225 in  
*Evolutionary Biology*, edited by M. K. Hecht, B. Wallace, and G. T. Prance. Springer  
1020 US, Boston, MA.
- Lack, J. B., C. M. Cardeno, M. W. Crepeau, W. Taylor, R. B. Corbett-Detig *et al.*, 2015 The  
1022 *Drosophila* Genome Nexus: A Population Genomic Resource of 623 *Drosophila*  
*melanogaster* Genomes, Including 197 from a Single Ancestral Range Population.  
1024 Genetics 199: 1229–1241.
- Lack, J. B., J. D. Lange, A. D. Tang, C.-D. B Russell, and J. E. Pool, 2016 A Thousand Fly  
1026 Genomes: An Expanded *Drosophila* Genome Nexus. Mol Biol Evol 33: 3308–3313.
- Langley, C. H., K. Stevens, C. Cardeno, Y. C. G. Lee, D. R. Schrider *et al.*, 2012 Genomic  
1028 variation in natural populations of *Drosophila melanogaster*. Genetics 192: 533–598.
- Li, H., 2013 Aligning sequence reads, clone sequences and assembly contigs with BWA-  
1030 MEM. Preprint: arXiv:1303.3997 [q-bio.GN].
- Li, H., 2011 Tabix: fast retrieval of sequence features from generic TAB-delimited files.  
1032 Bioinformatics 27: 718–719.
- Li, H., B. Handsaker, A. Wysoker, T. Fennell, J. Ruan *et al.*, 2009 The Sequence  
1034 Alignment/Map format and SAMtools. Bioinformatics 25: 2078–2079.



- Li, H., and W. Stephan, 2006 Inferring the Demographic History and Rate of Adaptive  
1036 Substitution in *Drosophila*. PLoS Genet 2: 10.
- Liao, J. J. Z., and J. W. Lewis, 2000 A Note on Concordance Correlation Coefficient. PDA J  
1038 Pharm Sci Technol 54: 23–26.
- Lin, L. I.-K., 1989 A Concordance Correlation Coefficient to Evaluate Reproducibility.  
1040 Biometrics 45: 255–268.
- Lynch, M., D. Bost, S. Wilson, T. Maruki, and S. Harrison, 2014 Population-Genetic  
1042 Inference from Pooled-Sequencing Data. Genome Biol Evol 6: 1210–1218.
- Machado, H. E., A. O. Bergland, K. R. O'Brien, E. L. Behrman, P. S. Schmidt *et al.*, 2016  
1044 Comparative population genomics of latitudinal variation in *Drosophila simulans* and  
*Drosophila melanogaster*. Mol Ecol 25: 723–740.
- Machado, H. E., A. O. Bergland, R. Taylor, S. Tilk, E. Behrman *et al.*, 2019 Broad  
1046 geographic sampling reveals predictable, pervasive, and strong seasonal adaptation  
1048 in *Drosophila*. Preprint: bioRxiv 337543.
- Mackay, T. F. C., S. Richards, E. A. Stone, A. Barbadilla, J. F. Ayroles *et al.*, 2012 The  
1050 *Drosophila melanogaster* Genetic Reference Panel. Nature 482: 173–178.
- Markow, T. A., and P. M. O'Grady, 2005 *Drosophila: a guide to species identification and*  
1052 *use*. Academic Press (Elsevier), Amsterdam, □ Boston.
- Martin, M., 2011 Cutadapt removes adapter sequences from high-throughput sequencing  
1054 reads. EMBnet.journal 17: 10–12.
- Mateo, L., G. E. Rech, and J. González, 2018 Genome-wide patterns of local adaptation in  
1056 Western European *Drosophila melanogaster* natural populations. Sci Rep 8: 16143.
- Mateo, L., A. Ullastres, and J. González, 2014 A transposable element insertion confers  
1058 xenobiotic resistance in *Drosophila*. PLoS Genet 10: e1004560.
- McKenna, A., M. Hanna, E. Banks, A. Sivachenko, K. Cibulskis *et al.*, 2010 The Genome  
1060 Analysis Toolkit: A MapReduce framework for analyzing next-generation DNA  
sequencing data. Genome Res 20: 1297–1303.
- Novembre, J., and M. Stephens, 2008 Interpreting principal component analyses of spatial  
1062 population genetic variation. Nat Genet 40: 646–649.
- Ometto, L., 2010 Inferring the Effects of Demography and Selection on *Drosophila*  
1064 *melanogaster* Populations from a Chromosome-Wide Scan of DNA Variation. Mol  
1066 Biol Evol 22: 2119–2130.
- Orozco-terWengel, P., M. Kapun, V. Nolte, R. Kofler, T. Flatt *et al.*, 2012 Adaptation of  
1068 *Drosophila* to a novel laboratory environment reveals temporally heterogeneous  
trajectories of selected alleles. Mol Ecol 21: 4931–4941.



- 1070 Paaby, A. B., A. O. Bergland, E. L. Behrman, and P. S. Schmidt, 2014 A highly pleiotropic  
amino acid polymorphism in the *Drosophila* insulin receptor contributes to life-history  
1072 adaptation. *Evolution* 68: 3395–3409.
- Paaby, A. B., M. J. Blacket, A. A. Hoffmann, and P. S. Schmidt, 2010 Identification of a  
1074 candidate adaptive polymorphism for *Drosophila* life history by parallel independent  
clines on two continents. *Mol Ecol* 19: 760–774.
- 1076 Pool, J. E., C.-D. B Russell, R. P. Sugino, K. A. Stevens, C. M. Cardeno *et al.*, 2012  
Population Genomics of Sub-Saharan *Drosophila melanogaster*: African Diversity  
1078 and Non-African Admixture. *PLoS Genet* 8: e1003080.
- Raineri, E., L. Ferretti, E.-C. Anna, B. Nevado, S. Heath *et al.*, 2012 SNP calling by  
1080 sequencing pooled samples. *BMC Bioinformatics* 13: 1–8.
- Ramaekers, A., A. Claeys, M. Kapun, E. Mouchel-Vielh, D. Potier *et al.*, 2019 Altering the  
1082 Temporal Regulation of One Transcription Factor Drives Evolutionary Trade-Offs  
between Head Sensory Organs. *Dev Cell* 50: 780-792.
- 1084 Reinhardt, J., B. Kolaczowski, C. Jones, D. Begun, and A. Kern, 2014 Parallel Geographic  
Variation in *Drosophila melanogaster*. *Genetics* 197: 361–373.
- 1086 Rodríguez-Trelles, F., R. Tarrío, and M. Santos, 2013 Genome-wide evolutionary response  
to a heat wave in *Drosophila*. *Biol Lett* 9: 20130228.
- 1088 Rudman, S. M., S. Greenblum, R. C. Hughes, S. Rajpurohit, O. Kiratli *et al.*, 2019  
Microbiome composition shapes rapid genomic adaptation of *Drosophila*  
1090 *melanogaster*. *Proc Natl Acad Sci USA* 116: 20025-20032.
- dos Santos, G., A. J. Schroeder, J. L. Goodman, V. B. Strelets, M. A. Crosby *et al.*, 2015  
1092 FlyBase: introduction of the *Drosophila melanogaster* Release 6 reference genome  
assembly and large-scale migration of genome annotations. *Nucleic Acids Res* 43:  
1094 D690–D697.
- Schlötterer, C., R. Tobler, R. Kofler, and V. Nolte, 2014 Sequencing pools of individuals -  
1096 mining genome-wide polymorphism data without big funding. *Nat Rev Genet* 15:  
749–763.
- 1098 Schneider, D., 2000 Using *Drosophila* as a model insect. *Nat Rev Genet* 1: 218–226.
- Sprengelmeyer, Q. D., S. Mansourian, J. D. Lange, D. R. Matute, B. S. Cooper *et al.*, 2020  
1100 Recurrent Collection of *Drosophila melanogaster* from Wild African Environments  
and Genomic Insights into Species History. *Mol Biol Evol* 37: 627–638.
- 1102 Stajich, J. E., and M. W. Hahn, 2005 Disentangling the Effects of Demography and Selection  
in Human History. *Mol Biol Evol* 22: 63–73.
- 1104 Stephan, W., 2016 Signatures of positive selection: from selective sweeps at individual loci  
to subtle allele frequency changes in polygenic adaptation. *Mol Ecol* 25: 79–88.

- 1106 Turner, T. L., M. T. Levine, M. L. Eckert, and D. J. Begun, 2008 Genomic Analysis of  
Adaptive Differentiation in *Drosophila melanogaster*. *Genetics* 179: 455–473.
- 1108 Turner, T. L., A. D. Stewart, A. T. Fields, W. R. Rice, and A. M. Tarone, 2011 Population-  
Based Resequencing of Experimentally Evolved Populations Reveals the Genetic  
1110 Basis of Body Size Variation in *Drosophila melanogaster*. *PLoS Genet* 7: e1001336.
- Umina, P. A., 2005 A Rapid Shift in a Classic Clinal Pattern in *Drosophila* Reflecting Climate  
1112 Change. *Science* 308: 691–693.
- Waldvogel, A.-M., B. Feldmeyer, G. Rolshausen, M. Exposito-Alonso, C. Rellstab *et al.*,  
1114 2020 Evolutionary genomics can improve prediction of species' responses to climate  
change. *Evol Lett* 4: 4–18.
- 1116 Wallace, M. A., K. A. Coffman, C. Gilbert, S. Ravindran, G. F. Albery *et al.*, 2020 The  
discovery, distribution and diversity of DNA viruses associated with *Drosophila*  
1118 *melanogaster* in Europe. *Virus Evolution*, in revision (preprint: bioRxiv  
2020.10.16.342956).
- 1120 Wittmann, M. J., A. O. Bergland, M. W. Feldman, P. S. Schmidt, and D. A. Petrov  
Seasonally fluctuating selection can maintain polymorphism at many loci via  
1122 segregation lift. *Proc Natl Acad Sci USA* 114: E9932–E9941.
- Wright, S., 1943 Isolation by distance. *Genetics* 28: 114.
- 1124 Zheng, X., S. M. Gogarten, M. Lawrence, A. Stilp, M. P. Conomos *et al.*, 2017 SeqArray - a  
storage-efficient high-performance data format for WGS variant calls. *Bioinformatics*  
1126 33: 2251–2257.
- Zhu, Y., A. O. Bergland, J. González, and D. A. Petrov, 2012 Empirical Validation of Pooled  
1128 Whole Genome Population Re-Sequencing in *Drosophila melanogaster*. *PLoS ONE*  
7: e41901.
- 1130